

Learning Personalized Decision Support Policies

Umang Bhatt^{1, 2, 3*}, Valerie Chen^{4*}, Katherine M. Collins¹, Parameswaran Kamalaruban², Emma Kallina^{1, 2}, Adrian Weller^{1, 2}, Ameet Talwalkar⁴

¹University of Cambridge
²The Alan Turing Institute
³New York University
⁴Carnegie Mellon University

Abstract

Individual human decision-makers may benefit from different forms of support to improve decision outcomes, but when each form of support will yield better outcomes? In this work, we posit that personalizing access to decision support tools can be an effective mechanism for instantiating the appropriate use of AI assistance. Specifically, we propose the general problem of learning a *decision support policy* that, for a given input, chooses which form of support to provide to decision-makers for whom we initially have no prior information. We develop *Modiste*, an interactive tool to learn personalized decision support policies. *Modiste* leverages stochastic contextual bandit techniques to personalize a decision support policy for each decision-maker and supports extensions to the multi-objective setting to account for auxiliary objectives like the cost of support. We find that personalized policies outperform offline policies, and, in the cost-aware setting, reduce the incurred cost with minimal degradation to performance. Our experiments include various realistic forms of support (e.g., expert consensus and predictions from a large language model) on vision and language tasks. Our human subject experiments validate our computational experiments, demonstrating that personalization can yield benefits in practice for real users, who interact with *Modiste*.

Introduction

To improve decision outcomes, human decision-makers can use various forms of support to inform their opinions before making a final decision (Keen 1980). Decision-makers with differing expertise may benefit from different forms of support on a given input. For example, one radiologist may provide a better diagnosis of a chest X-ray by leveraging model predictions (Kahn Jr 1994) while another may perform better after viewing suggestions from senior radiologists (Briggs et al. 2008): see Figure 1. In this paper, we study how to improve decision outcomes by *personalizing* which form of support we provide to a decision-maker on a case-by-case basis.

Since artificial intelligence (AI) is increasingly used as a form of decision support (Lai et al. 2023), responsible machine learning (ML) model deployment requires clarity on

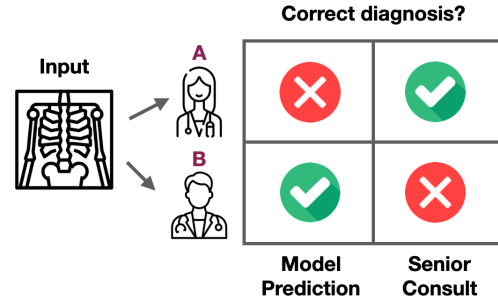


Figure 1: Depending on the input, decision-makers need different forms of decision support to make correct decisions. *Modiste* personalizes access to the right form of support at the right time for the right decision-maker. Here, Alice would not benefit from model access, while Bob would not benefit from a senior consult.

who should have access to model outputs and when model outputs can be safely exposed to decision-makers (Amodei et al. 2016). Regulation increasingly calls for the “effective and appropriate use” of AI (Biden 2023), requiring careful consideration of when models ought to be accessible to decision-makers. In this paper, we formalize learning a *decision support policy* that dictates for each individual decision-maker when additional support (e.g., LLM output) should be viewed and used for a given input.

While prior work has assumed access to offline human decisions under support (Laidlaw and Russell 2021; Charusaie et al. 2022) or oracle queries of human behavior (De-Arteaga, Dubrawski, and Chouldechova 2018; Mozannar and Sontag 2020) to learn decision support policies, we argue that this data is unrealistic to obtain in practice across all available forms of support *for a new decision-maker*. Thus, for individuals for whom we have no prior information initially, we propose learning how to personalize support *online*. We develop *Modiste*,¹ an interactive tool that leverages off-the-shelf stochastic contextual bandit algorithms (Li et al. 2010) to learn decision support policies. Since providing support may

*Both authors contributed equally. Order was decided by a coin flip. Please direct correspondence to: valeriechen@cmu.edu and umangbhatt@nyu.edu

¹While a “modiste” usually refers to someone who tailors clothing and makes dresses/hats, we use the term to capture our tool’s ability to alter a policy to a decision-maker.

be costly (Arbiser, Folpe, and Weiss 2001; Mimra, Rasch, and Waibel 2016), we incorporate a second objective, the cost of support, and implement mechanisms for trading-off performance and cost when using `Modiste`.

Our computational experiments explore the utility of personalization in both the cost-agnostic and cost-aware settings. Based on these experiments, we characterize decision-maker expertise into profiles where personalized policies outperform offline ones. We demonstrate that if there is no benefit of personalization, `Modiste` recovers fixed policies, which always provide one form of support. In the cost-aware setting, we show that personalization can reduce the incurred cost with minimal degradation to performance.

To validate `Modiste` on real users ($N = 125$), we conduct human subject experiments, where we explore forms of support that include expert consensus, outputs from an LLM, or predictions from a classification model. In contrast to prior work that only tests offline policies or evaluates in simulation, we demonstrate how `Modiste` can be used to learn personalized decision support policies online on both vision and language tasks. We emphasize our main contributions:

1. Formalizing decision support policies. We propose a formulation for learning a personalized decision support policy that selects the form of support that maximizes a given decision-maker’s performance. We introduce `Modiste`, a tool to instantiate our formulation using existing methods from stochastic contextual bandits, and provide a multi-objective extension to incorporate the cost of support. We open-source `Modiste` as a tool to encourage the adoption of personalized decision support policies.

2. Evaluating personalized policies in realistic settings. We demonstrate the importance of online learning to personalize policies for new decision-makers through both computational and human subject experiments on vision and language tasks. We characterize under which settings we would expect personalized policies to improve performance and/or cost. Our human subject experiments, where real users interact with `Modiste`, validate our findings from the computational experiments on synthetic decision-makers, demonstrating the benefits of personalized policies in practice.

Related Work

Regulating AI Use. Our study of decision support policies has implications for safely deploying ML models to interact with users. This topic is of heightened importance, particularly in light of recent calls for the “effective and appropriate use” of AI in US President Biden’s Executive Order (Biden 2023) and for clarity on when to “decide not to use [an] AI system” per the EU AI Act (EUA 2023). The disuse of AI can caution downstream misuse of models for assistive decision-making (Brundage et al. 2018). The refusal to use AI assistance can be strategic to empower decision-makers, thus preventing their overreliance on models and encouraging their agency on the task at hand (Gordon and Mugar 2020; Barabas 2022). Each decision-maker may require a different level of use to promote effective use of AI assistance in their decision-making (Kirk et al. 2024); for instance, experts and novices may prefer LLM access in different settings on theorem proving tasks (Collins et al. 2023b). Our experiments

engage with such settings by learning when to provide LLM support for language-based tasks via a personalized policy.

Decision Support. While various forms of decision support have been proposed, such as expert consensus (Scheife et al. 2015) and changes to machine interfaces (Roda 2011), more recent forms of support focus on algorithmic tools where decision-makers are aided by machine learning (ML) models (Phillips-Wren 2012; Gao et al. 2021; Bastani, Bastani, and Sinchaisri 2022). In some prior work, the human does not always make the final decision, such as those that learn to defer decisions from a model to a single decision-maker (Madras, Pitassi, and Zemel 2018; Mozannar and Sontag 2020) or others that jointly learn an allocation function between a model and a pool of decision makers (Keswani, Lease, and Kenthapadi 2021; Hemmer et al. 2022). In our setting, the *human* is always the decision-maker, even after viewing any form of support: this reflects many real-world applications. This setting includes ones where humans make the final decisions with support from ML models (Green and Chen 2019; Lai et al. 2023), as well as ones where humans make decisions when provided with additional information beyond a model prediction, e.g., explanations (Bansal et al. 2021b), uncertainty (Zhang, Liao, and Bellamy 2020), conformal sets (Babbar, Bhatt, and Weller 2022). While these studies *always* show a single form of support, recent works consider adapting when AI support is shown to users with a fixed policy. Ma et al. (2023) fit a decision tree to offline user’s decisions to decide when to show AI support to users, and Buçinca et al. (2024) use offline reinforcement learning to estimate if AI support would be helpful, especially under time constraints (Swaroop et al. 2024). Our work considers general forms of support, beyond when to show AI support, and formalizes *learning* in which contexts each form of support should be provided to an unseen decision-maker online. An extensive comparison to prior work is in the Appendix.

Prior Assumptions About Decision-Maker Information. We briefly survey the assumptions made about the decision-maker when learning decision support policies. The model of the decision maker is either synthetic, thus lacking grounding in actual human behavioral data, or learned from a batch of *offline* annotations (Madras, Pitassi, and Zemel 2018; Okati, De, and Rodriguez 2021; Charusaie et al. 2022; Gao et al. 2023). For a new decision-maker or a new form of support, this set of data would not be available in practice. Instead, we propose to learn a decision support policy *online* to circumvent these limitations. Few works use some aspect of online learning for different decision-making settings or under strict theoretical conditions, as we describe in the Appendix.

Preliminaries

We consider a human decision-making process with different forms of decision support. In our setting, decision-makers may be shown support when selecting an outcome from a fixed set of labels (Seger and Peterson 2013; Lai et al. 2023).

General Problem Formulation. Decision-makers perform a classification task in observation/feature space $\mathcal{X} \subseteq \mathbb{R}^p$ and

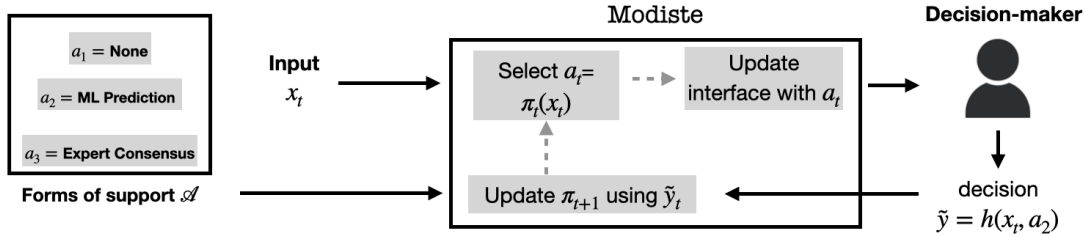


Figure 2: We illustrate the process of learning a decision support policy π_t online to improve a decision-maker h 's performance. Without assuming access to prior offline data, our formulation learns a personalized policy *online*; each decision-maker's learned policy may differ from that of another decision-maker if they have decisions (\tilde{y}) and thus different expertise. We also consider a cost-aware version of this learning problem that modifies how a_t is selected.

outcome/label space $\mathcal{Y} = [K]$. We operate in a stochastic setting where the data $(x, y) \in \mathcal{X} \times \mathcal{Y}$ are drawn iid from a fixed, unknown data generating distribution \mathcal{P} , an assumption that reflects typical decision-making settings (Bastani and Bayati 2020; Bastani, Bastani, and Sinchaisri 2022). Importantly, we consider an action set \mathcal{A} corresponding to the forms of support available, which may consist of an individual piece of information (e.g., model prediction) or a particular combination of multiple pieces of information (e.g., model prediction and explanation). Given an observation $x \in \mathcal{X}$, the human attempts to predict the corresponding label $y \in \mathcal{Y}$ using the support prescribed by an action $a \in \mathcal{A}$. Note, we do not make assumptions on the specific forms of support a , but we provide multiple instantiations in our experiments. The quality of predictions is measured using a 0-1 loss function, where $\ell(y, y') = 1$ for $y \neq y'$ and $\ell(y, y') = 0$ for $y = y'$.

Decision-Making Protocol. A personalized decision support policy $\pi : \mathcal{X} \rightarrow \Delta(\mathcal{A})$ outputs a form of support for a given input. Let Π denote the class of all stochastic decision support policies. Let $\mathcal{A} = \{A_1, \dots, A_k\}$, and $\pi(x)_{A_i}$ denote $\mathbb{P}[A_i \sim \pi(x)]$ for each $A_i \in \mathcal{A}$. When the policy π prescribes the support A_i , the human decision-maker makes the prediction \tilde{y} based on the observation x and support A_i , i.e., the final prediction \tilde{y} is given by $\tilde{y} = h(x, A_i)$. The human decision-making process with different forms of support is described below. For $t = 1, 2, \dots, T$:

1. A data point $(x_t, y_t) \in \mathcal{X} \times \mathcal{Y}$ is drawn iid from \mathcal{P} .
2. A form of support $a_t \in \mathcal{A}$ is selected using a decision support policy $\pi_t : \mathcal{X} \rightarrow \Delta(\mathcal{A})$.
3. The human decision-maker makes the final prediction $\tilde{y}_t = h(x_t, a_t)$ based on x_t and a_t .
4. The human decision-maker incurs a loss $\ell(y_t, \tilde{y}_t) = 1$ if $y_t \neq \tilde{y}_t$ and $\ell(y_t, \tilde{y}_t) = 0$ otherwise.

A static decision support policy would not change throughout the interaction with the decision-maker. This reflects many prior user studies, per Lai et al. (2023); for example, decision-makers may *always* be presented with model predictions. We iteratively update π at each time step to personalize the policy based on the decision-maker's most recent prediction.

Evaluation of π via Expected Loss. The quality of a policy π can be evaluated using the expected loss incurred by the

decision-maker across the input space:

$$L_h(\pi) = \mathbb{E}_{(x,y) \sim \mathcal{P}} [\mathbb{E}_{A_i \sim \pi(x)} [\ell(y, h(x, A_i))]]. \quad (1)$$

We distinguish this metric from the more standard notion of regret, which is typically used to analyze policies in an online learning setting (Li et al. 2010); however, we cannot realize π^* for an unseen decision-maker in practical scenarios. Thus, we rely on $L_h(\cdot)$ as a proxy metric for evaluating the effectiveness of π .

Modiste: Learning Personalized Decision Support Policies

We introduce `Modiste`, a tool to translate our problem formulation into an interactive interface for learning personalized policies. The workflow, outlined in Figure 2, comprises a learning component to update the personalized policy and an interface to customize the appropriate form of support for each input and each decision-maker.

Learning Problem

The human decision-making process with various forms of support can be modeled as a stochastic contextual bandit problem, where the forms of support are the arms and \mathcal{X} is the context space. In Algorithm 1, we outline an online algorithm for learning the policy π^* that minimizes expected loss. In the cost-agnostic setting, our goal is to find an optimal decision support policy π^* that minimizes $L_h(\pi)$. We can rewrite Eq. 1 as follows:

$$L_h(\pi) = \mathbb{E}_x \left[\sum_{i=1}^k \pi(x)_{A_i} \cdot r_{A_i}(x; h) \right],$$

where $r_{A_i}(x; h) = \mathbb{E}_{y|x} [\ell(y, h(x, A_i))]$ is the human prediction error for input x and support A_i . Then, it can be shown that the optimal policy takes the form $\pi^*(x) = \arg \min_{A_i \in \mathcal{A}} r_{A_i}(x; h)$: see derivation in Appendix. For `Modiste` to run, we must maintain and update our estimate of human prediction error $r_{A_i}(x; h)$ (Step 1 in Algorithm 1) and of our policy π (Step 2 in Algorithm 1)

To update the estimate of human prediction error (Step 1), `Modiste` implements two approaches to estimate $r_{A_i}(x; h)$ for all $x \in \mathcal{X}$ and $A_i \in \mathcal{A}$, but note that any online learning algorithm can be used to update the \mathcal{U}_r . We first consider

LinUCB (Li et al. 2010), a common online learning algorithm that approximates the expected loss $r_{A_i}(x; h)$ by a linear function $\hat{r}_{A_i}(x; h) := \langle \theta_{A_i}, x \rangle$. Although the linearity assumption may not hold in general, we learn the parameters $\{\theta_{A_i} : A_i \in \mathcal{A}\}$ using LinUCB with the instantaneous reward function $R(x, y, A_i; h) := -\ell(y, h(x, A_i))$. We then normalize the resulting $\hat{r}_{A_i}(x; h)$ values to lie in the range $[0, 1]$. The second algorithm we use is an intuitive K -nearest neighbor (**KNN**) approach, which is a simplified variant of KNN-UCB (Guan and Jiang 2018). Here, we maintain an evolving data buffer \mathcal{D}_t , which accumulates a history of interactions with the decision-maker. For any new observation x , we estimate $\hat{r}_{A_i}(x; h)$ values by finding K -nearest neighbors in \mathcal{D}_t and computing the average error of these neighbors.

In practical settings where interactions are limited (like in our human subject experiments), the number of interactions T tends to be relatively small, which renders pure exploratory policies infeasible (Sutton and Barto 2018). Thus in Step 2, we guide exploration of the policy via:

$$\pi_{t+1}(x) = \arg \min_{A_i \in \mathcal{A}} \hat{r}_{A_i, t}(x; h) + b_{A_i, t}(x; h),$$

where $b_{A_i, t}(x; h)$ corresponds to some exploration bonus. In the Appendix, we provide implementations of `Modiste` with LinUCB (Algorithm 2) and KNN (Algorithm 3).

Algorithm 1: Learning a decision support policy

- 1: **Input:** human decision-maker h
 - 2: **Initialization:** data buffer $\mathcal{D}_0 = \{\}$; human error values $\{\hat{r}_{A_i, 0}(x; h) = 0.5 : x \in \mathcal{X}, A_i \in \mathcal{A}\}$; initial policy π_1
 - 3: **for** $t = 1, 2, \dots, T$ **do**
 - 4: data point $(x_t, y_t) \in \mathcal{X} \times \mathcal{Y}$ is drawn iid from \mathcal{P}
 - 5: support $a_t \in \mathcal{A}$ is selected using policy π_t
 - 6: human makes the prediction \tilde{y}_t based on x_t and a_t
 - 7: human incurs the loss $\ell(y_t, \tilde{y}_t)$
 - 8: update the buffer $\mathcal{D}_t \leftarrow \mathcal{D}_{t-1} \cup \{(x_t, a_t, \ell(y_t, \tilde{y}_t))\}$
 - 9: update the decision support policy:

$$\hat{r}_{A_i, t}(x; h) \leftarrow \mathcal{U}_r(\hat{r}_{A_i, t-1}(x; h), \mathcal{D}_t), \quad \forall A_i \in \mathcal{A} \quad (\text{Step 1})$$

$$\pi_{t+1}(x) \leftarrow \mathcal{U}_\pi(\{\hat{r}_{A_i, t}\}_i) \quad (\text{Step 2})$$
 - 10: **end for**
 - 11: **Output:** policy $\pi_\lambda^{\text{alg}} \leftarrow \pi_{T+1}$
-

Extension to Cost-Aware Decision Support. Providing decision support can be expensive (Arbiser, Folpe, and Weiss 2001; Mimra, Rasch, and Waibel 2016), so in addition to minimizing loss, it may be desirable to minimize the cost of providing support. We quantify the expected cost of a policy π using $c(\pi) = \mathbb{E}_x \left[\sum_{i=1}^k \pi(x)_{A_i} \cdot c(A_i) \right]$, where $c(A_i)$ is the cost of providing support A_i . We reformulate our objective as $\pi_\lambda^* = \arg \min_{\pi \in \Pi} \lambda \cdot L_h(\pi) + (1 - \lambda) \cdot c(\pi)$, where $\lambda \in [0, 1]$. Since $c(A_i)$ does not depend on x , it does not affect Step 1. Specifically, we can update Step 2 of Algorithm 1 to the following:

$$\pi_{t+1}(x) = \arg \min_{A_i \in \mathcal{A}} \lambda \cdot \hat{r}_{A_i, t}(x; h) + (1 - \lambda) \cdot c(A_i) + b_{A_i, t}(x; h).$$

In practice, it may be unclear how to select λ , but one way to consider this problem may be to learn a decision support policy π that achieves a certain level of performance at a minimal cost: given a tolerance threshold $\epsilon \in [0, 1]$ for the expected loss, we can find a policy π that achieves the minimum expected cost while maintaining the expected loss $L_h(\pi)$ within ϵ of the optimal loss L_h^{opt} , where $L_h^{\text{opt}} = \min_{\pi} L_h(\pi)$. Given a large number of interactions with a decision-maker h , we can simply run Algorithm 1 for multiple values of λ , i.e., sampling from $\lambda \in [0, 1]$. From the set of corresponding policies learned for each λ , we can evaluate which λ yields a policy with the lowest cost within ϵ of L_h^{opt} .

For a new decision-maker, it is often infeasible to extensively test many choices of λ values simultaneously without repeating queries of the same input (e.g., as in our human subject experiments); thus, we leverage a hyper-parameter tuning strategy using population data. We follow the above workflow to find suitable values for λ for each decision-maker in a population. From this set of candidate λ values, we select a λ to deploy by choosing the most common value (mode) of all λ values that yield policies which get decision-makers within ϵ of their optimal loss. Although the decision-makers in the population may differ from the unseen decision-maker, we prefer this to a random selection of λ at deployment.

Modiste Interface

We provide an extendable interface for the study and deployment of decision-support policies. At each time step, `Modiste` sends each user’s predictions to a server running Algorithm 1, which identifies the next form of support for the next input. `Modiste` then updates the interface accordingly to reflect the selected form of support. Our tool can flexibly be linked with crowdsourcing platforms like Prolific (Palan and Schitter 2018). We implement three common forms of support: (1) `HUMAN ALONE`, where the human makes the decision solely based on the input, (2) `MODEL PREDICTION`, which shows decision-makers a model’s prediction for the given input (Bastani, Bastani, and Sinchaisri 2022), and (3) `EXPERT CONSENSUS`, which presents the user with a distribution over labels from multiple annotators (Scheife et al. 2015). In Figure 3, we provide screenshots of the interface under each form of support. Participants are informed of their own correctness after each trial, as well as the correctness of the form of support (e.g., model prediction), if support was provided, so that participants can learn whether support ought to be relied upon.

Experimental Set-up

Before we validate `Modiste`, we overview the set-up of subsequent experiments, both computational and human subject. All other details are in the Appendix.

Decision-making Tasks

Following prior studies on human-AI interactions (Babbar, Bhatt, and Weller 2022; Mozannar et al. 2023; Lee et al. 2023), the decision-making tasks in our experiments center around the following vision and language datasets:

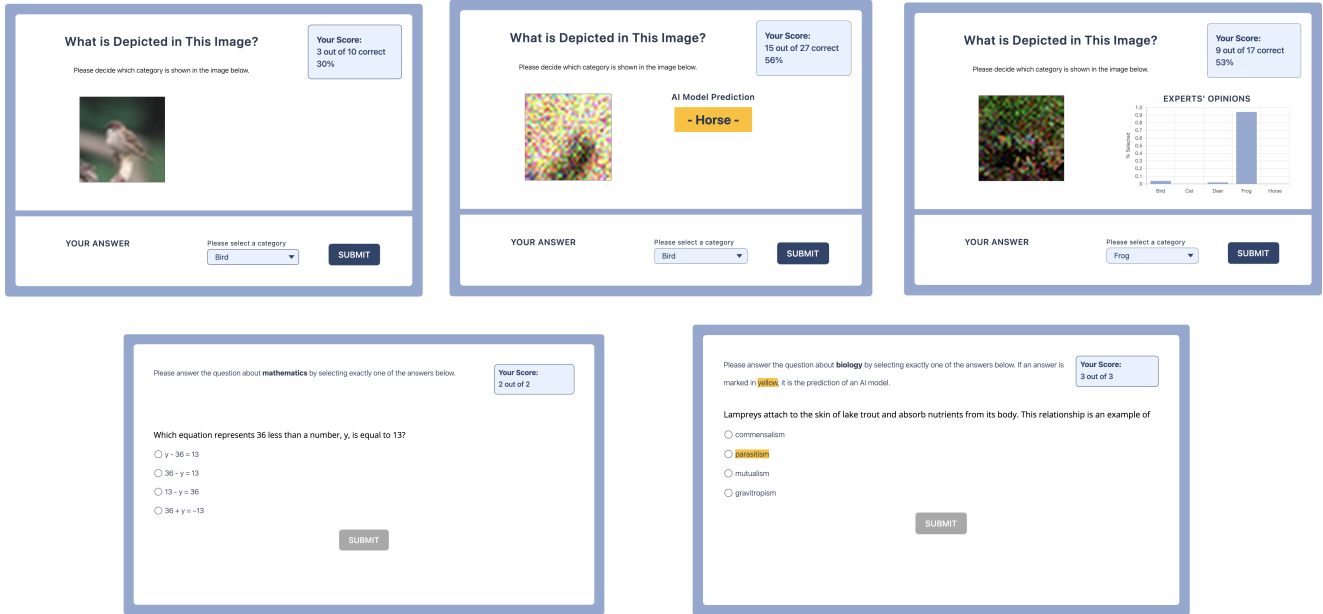


Figure 3: Examples of the `Modiste` interface for each form of support in `CIFAR-3A` (Top) and `MMLU-2A` (Bottom). From left to right, top row: `HUMAN ALONE`, `MODEL`, and `CONSENSUS`; bottom row: `HUMAN ALONE` and `LLM`.

1. `CIFAR-10` (Krizhevsky 2009), a 10-class image classification dataset;
2. `MMLU` (Hendrycks et al. 2020), a multi-task text-based benchmark that tests for knowledge and problem-solving ability across 57 topics in both the humanities and STEM.

In terms of the size of $|\mathcal{A}|$, we let kA denote when there are k forms of support for a task. We focus on $k = 2$ or 3 , which captures a buffet of real-world scenarios in prior work where decision-makers have a few tools at their disposal. In particular, the two action setting covers practical use cases where a decision-maker has the option of using a model or not. The learned decision support policy then reflects appropriate use, as the model would be hidden when a decision-maker does not need it. While the forms of support we consider are common in practice (Lai et al. 2023), our choices of support are not intended to exhaustively demonstrate the diverse forms of support that `Modiste` can handle. We now describe our two main tasks, which are designed to be accessible to crowdworkers and will be featured in both the computational and human subject experiments.²

CIFAR-3A. In this task, we consider three forms of support: `HUMAN ALONE`, `MODEL`, `CONSENSUS`. Our goal is to construct a setup reflecting a realistic setting in which different forms of support result in different strengths and weaknesses for decision-makers. To instantiate this setting, we deliberately corrupt images of different classes to evoke performance differences – necessitating that a decision-maker

²In the Appendix, we include computational experiments for two additional tasks (`Synthetic-2A` and `CIFAR-2A`), and experiments where we vary the size of k .

appropriately calibrate when to rely on each form of support. We consider 5 of the animal classes in `CIFAR-10`; of these, we never corrupt images of Birds, do not corrupt images of Deers and Cats for the `MODEL`, and do not corrupt images of Horses and Frogs for the `CONSENSUS`. We assume the cost of `HUMAN ALONE` is less than the cost of either form of support, and the cost of `MODEL` and `CONSENSUS` is equal.

MMLU-2A. The two forms of support are `HUMAN ALONE` and `LLM`, where the human is provided responses generated from `InstructGPT3.5`, `text-davinci-003`, (Ouyang et al. 2022) using the same few-shot prompting scheme for `MMLU` as Hendrycks et al. (2020). We conducted pilot studies to select a subset of topics where the accuracy of the LLM and average human accuracy vary. We choose the following topics: Computer Science, US Foreign Policy, High School Biology, and Elementary Mathematics. The goal of this task is to evaluate whether we can learn personalized support “*in-the-wild*,” where we naturally expect people to excel at different topics, akin to real-world settings where decision-makers may have varying expertise. Again, the cost of `MODEL` is greater than the cost of `HUMAN ALONE`.

Baselines and Other Parameters

Algorithms and Baselines. We compare personalized policies, learned using Algorithm 1 with `LinUCB` and with `KNN` reporting results as `Modiste-LinUCB` and `Modiste-KNN` respectively, against the following offline policies:

- *Human + Support*, where the decision-maker *always* receives the same form of support: $\pi(x) = A_i$ for all x . In `CIFAR-3A`, there are 3 fixed support baselines, correspond-

ing to each form of support. In MMLU-2A, there are 2 fixed support baselines.

- *Population-level*, where the decision-maker receives a form of support based on the majority vote from 10 learned policies (breaking ties at random). For this baseline, the form of support may vary across contexts but is not personalized to individual needs. This baseline is akin to recent offline policy learning (Ma et al. 2023; Bućinca et al. 2024).

Number of Interactions. While more interactions (higher T) provide more data points to estimate each r_{A_i} , we need to consider what a realistic value of T is given constraints of working with real humans (e.g., limited attention and cognitive load). In online learning, T is usually unreasonably large, on the order of thousands (Li et al. 2010; Guan and Jiang 2018). Via pilot studies, we found that 100 CIFAR images or 60 MMLU questions were a reasonable number of decisions to make within 20-40 minutes (a typical time limit for an online study), which we use throughout our experiments.

Computational Validation

To validate `Modiste` computationally, we need access to simulated human behavior. Decision-makers may have different “expertise” (i.e., strengths and weaknesses) across input space \mathcal{X} under each form of support. To construct realistic synthetic decision-makers, we set up a pilot study to understand these differences. This allows us to see how expertise varies across decision-makers and identify the personalized policy we can expect `Modiste` to learn.

Expertise Profiles

We can capture an individual h ’s expertise via an *expertise profile*, which is defined over the input space \mathcal{X} . We divide \mathcal{X} into disjoint regions (i.e., $\mathcal{X} = \cup_{j \in [N]} \mathcal{X}_j$); these regions could be defined by class labels or by covariates, depending on the task.³ We let $r_{A_i}(\mathcal{X}_j; h)$ denote h ’s average prediction error under support A_i across region \mathcal{X}_j .

Human-informed synthetic decision-makers. To construct expertise profiles with *realistic* values for each $r_{A_i}(\mathcal{X}_j; h)$, we collect data on user decisions across different users and then calculate individual $r_{A_i}(\mathcal{X}_j; h)$. The set of participant expertise profiles form a population of decision-makers that we refer to as *human-informed synthetic decision-makers*. From the estimated $r_{A_i}(\mathcal{X}_j; h)$ of each human-informed synthetic decision-maker, we can simulate decision-maker behavior. We leverage these decision-makers to evaluate multiple values of λ in our computational experiments and to select λ values to deploy on unseen decision-makers in our human subject experiments.

To construct human-informed synthetic decision-makers, we recruited 20 participants from Prolific (10 for CIFAR-3A and 10 for MMLU-2A). We use the same recruitment scheme as the larger human subject experiment described in the Appendix. We define regions of expertise over class

³While we instantiate decision-makers this way, `Modiste` does not take the expertise profiles or how they were constructed (e.g., the regions) as input.

labels for CIFAR-3A and over question topics for MMLU-2A, as we expect $r_{A_i}(x; h)$ to be roughly constant for $x \in \mathcal{X}_j$ where \mathcal{X}_j is defined by a class label or question topic. We showed each participant similar inputs with different forms of support to estimate $r_{A_i}(\mathcal{X}_j; h)$ for each support A_i in each region \mathcal{X}_j . On each trial, each participant is randomly assigned a form of support; trials are approximately balanced by the type of support and grouping (i.e., topic or class). We compute participant accuracy averaged over all trials: 100 for CIFAR-3A, 60 for MMLU-2A. We denote expertise profiles in subsequent experiments as follows: if there were three regions in the input space, an individual’s expertise profile under support A_i would be written as $r_{A_i} = [0.7, 0.1, 0.7]$, meaning the individual incurs a loss of 0.7 on \mathcal{X}_1 , 0.1 on \mathcal{X}_2 , and 0.7 on \mathcal{X}_3 .

Policies for each profile. Based our pilot study, we define the three expertise profiles and what kind of decision support policy we expect to be learned for each:

- **Approximately Invariant** expertise across all the regions under different forms of support, i.e., $r_{A_1}(\mathcal{X}_j; h) \approx r_{A_2}(\mathcal{X}_j; h) \approx \dots \approx r_{A_k}(\mathcal{X}_j; h), \forall j \in [N]$. In the cost-aware setting, a decision support policy should learn the fixed form of support that corresponds to picking the cheapest form of support.
- **Varying** expertise where a decision-maker excels in some areas but benefits from support in areas beyond their training (Schvaneveldt et al. 1985), i.e., $r_{A_1}(\mathcal{X}_j; h) \leq r_{A_2}(\mathcal{X}_j; h)$ and $r_{A_2}(\mathcal{X}_k; h) \leq r_{A_1}(\mathcal{X}_k; h)$, for some $j, k \in [N]$. For this expertise profile, we expect the decision support policy to select different forms of support in different regions. The quantity of $|r_{A_1} - r_{A_2}|$ for a region will dictate how efficiently the policy can be learned.
- **Strictly Better** expertise (e.g., $A_1 \succ A_2 \succ \dots \succ A_k$) that is uniformly maintained across all the regions, i.e., $r_{A_1}(\mathcal{X}_j; h) \leq r_{A_2}(\mathcal{X}_j; h) \leq \dots \leq r_{A_k}(\mathcal{X}_j; h), \forall j \in [N]$. A decision support policy should learn the fixed form of support to use for all inputs.

Per the task design, we find participants generally only display varying expertise profiles on CIFAR-3A while we find instances of all three expertise profiles on MMLU-2A.

When is personalization useful?

We use human-informed synthetic decision-makers to evaluate `Modiste` in both cost-agnostic and cost-aware settings.

Cost-agnostic results. We investigate how personalized policies compare against offline baselines under each expertise profile (Table 1). We verify that learning decision support policies are not helpful for decision-makers with “invariant” expertise profiles. However, for individuals who fall under the “strictly better” and “varying” profiles, we find at least one personalized policy outperforms offline policies and learns a policy that is closer to the decision-maker’s optimal performance. This is because a personalized policy identifies *which* form of support is better in each context, compared to fixed offline policies which *always* show one form of support or to the population variant, which may not provide the correct

Table 1: In the cost-agnostic setting, we evaluate the average excess loss $L_h(\pi) - L_h^{opt}$ (lower is better), and standard deviation across individuals in each expertise profile for both CIFAR-3A (Left) and MMLU-2A (Right). $L_h(\pi)$ is computed by averaging across the last 10 steps of 100 total time steps. We **bold** the variant with the lowest excess loss.

Algorithm	Invariant	Strictly Better	Varying
H-ONLY	0.00 ± 0.01	0.09 ± 0.08	0.50 ± 0.06
H-MODEL	0.00 ± 0.01	0.22 ± 0.19	0.35 ± 0.05
H-CONSENSUS	0.00 ± 0.01	0.23 ± 0.13	0.27 ± 0.08
Population	0.00 ± 0.02	0.18 ± 0.08	0.15 ± 0.03
Modiste-LinUCB	0.00 ± 0.01	0.17 ± 0.05	0.19 ± 0.05
Modiste-KNN	0.00 ± 0.01	0.06 ± 0.01	0.08 ± 0.02

Algorithm	Invariant	Strictly Better	Varying
H-ONLY	0.01 ± 0.01	0.18 ± 0.17	0.22 ± 0.12
H-LLM	0.01 ± 0.01	0.18 ± 0.21	0.12 ± 0.17
Population	0.00 ± 0.02	0.19 ± 0.07	0.12 ± 0.09
Modiste-LinUCB	0.00 ± 0.01	0.12 ± 0.03	0.07 ± 0.04
Modiste-KNN	0.01 ± 0.01	0.05 ± 0.03	0.05 ± 0.03

Table 2: In the cost-aware setting for MMLU-2A, we compare the expected loss $L_h(\pi)$ and the expected cost $c(\pi)$ (lower is better) averaged across the last 10 steps of 100 total time steps of 5 separate runs. We select two individuals who have a “varying” profile and two individuals who have a “strictly better” profile. We follow the described workflow to find a suitable λ , reported for each person in Table 5. We **bold** the algorithm that achieves the lowest cost within $\epsilon = 0.05$ risk of each individual h ’s L_h^{opt} .

Algorithm	Varying: $L_h^{opt} = 0.13$		Varying: $L_h^{opt} = 0.10$		Strictly Better: $L_h^{opt} = 0.43$		Strictly Better: $L_h^{opt} = 0.09$	
	$r_{H-ONLY} = [0.3, 0.1, 0.5, 0.3]$	$r_{H-LLM} = [0.5, 0.1, 0.0, 0.1]$	$r_{H-ONLY} = [0.1, 0.3, 0.6, 0.6]$	$r_{H-LLM} = [0.4, 0.0, 0.3, 0.0]$	$r_{H-ONLY} = [0.8, 0.6, 0.8, 0.6]$	$r_{H-LLM} = [0.6, 0.3, 0.7, 0.1]$	$r_{H-ONLY} = [0.3, 0.9, 0.3, 0.9]$	$r_{H-LLM} = [0.0, 0.1, 0.0, 0.3]$
	$L_h(\pi)$	$c(\pi)$	$L_h(\pi)$	$c(\pi)$	$L_h(\pi)$	$c(\pi)$	$L_h(\pi)$	$c(\pi)$
H-ONLY	0.30 ± 0.03	0.0	0.41 ± 0.04	0.0	0.68 ± 0.03	0.0	0.54 ± 0.05	0.0
H-LLM	0.21 ± 0.03	0.1	0.16 ± 0.04	0.1	0.42 ± 0.06	0.1	0.09 ± 0.02	0.1
Population	0.13 ± 0.03	0.05 ± 0.01	0.16 ± 0.04	0.05 ± 0.01	0.53 ± 0.05	0.05 ± 0.01	0.35 ± 0.07	0.05 ± 0.01
Modiste-LinUCB	0.15 ± 0.05	0.04 ± 0.01	0.15 ± 0.04	0.06 ± 0.01	0.51 ± 0.06	0.06 ± 0.01	0.20 ± 0.10	0.06 ± 0.01
Modiste-KNN	0.17 ± 0.03	0.03 ± 0.01	0.15 ± 0.04	0.07 ± 0.01	0.46 ± 0.05	0.05 ± 0.02	0.12 ± 0.03	0.08 ± 0.01

form of support to each individual. We note that KNN generally outperforms LinUCB, the latter of which can be saddled by its implicit linearity assumption.

Cost-aware results. When accounting for both performance and cost of support, we aim to learn low-cost policies for each decision-maker that are within $\epsilon = 0.05$ of their optimal loss L_h^{opt} . In these experiments, we focus on MMLU-2A, where individuals naturally have “varying” and “strictly better” expertise profiles, two settings it makes sense to consider both loss and cost objectives (Table 2). We omit the “invariant” profile as the best policy is to simply select the cheapest form of support. For individuals who are “strictly better,” it may not be possible to further reduce the expected loss compared to one of the offline policies; however, we find that personalization can reduce cost while still achieving an expected loss that is within ϵ of L_h^{opt} . For the individuals with “varying” profiles, we find that personalization can improve both performance and cost over many of the offline baselines. We find the population baseline is inconsistent in its ability to identify high-performing policies at low cost, in contrast to the personalized policies learned. We report similar results for multiple datasets in the Appendix.

Selecting hyper-parameters. In the cost-aware setting, we used the human-informed synthetic decision-makers to learn policies for multiple values of λ simultaneously. However, we observe that often only a subset of the learned policies fall within ϵ of L_h^{opt} (e.g., in Figure 8), underscoring that it may be challenging to consistently select a suitable λ in practice. We further study the effect of various parameters, e.g., exploration parameters, KNN parameters, embedding size, and the number of interactions in the Appendix.

Modiste with real users

To validate whether Modiste can improve decision-maker performance and cost in practice, we run a series of human subject experiments (i.e., ethics-reviewed studies with real human participants). We first introduce the set-up of our user study; additional information can be found in the Appendix. To our knowledge, we are one of the first works that run actual user studies to demonstrate the benefits of learning personalized policies online: see an extensive comparison to prior work in the Appendix.

Recruitment. We recruit a total of 125 crowdsourced participants from Prolific to interact with Modiste ($N = 45$ and $N = 80$ for CIFAR-3A and MMLU-2A, respectively). We recruit more participants for MMLU-2A, as we expect greater individual differences in regions where support is needed, e.g., some participants may be good at mathematics and struggle in biology, whereas others may excel in biology questions, whereas in CIFAR-3A, there is an “optimal” form of support for each stimulus.

Each participant is assigned to only one task. Within a task, participants are randomly assigned to one algorithm variant; an equal number of participants are included per variant (i.e., 10 for MMLU and 5 for CIFAR). Participants are required to reside in the United States and speak English as a first language. Participants are paid at a base rate of \$9/hr, and are told they may be paid an optional bonus up to \$10/hr based on the number of correct responses. We allot 25-30 minutes for the CIFAR task and 30-40 for MMLU, as each MMLU question takes more effort. We applied the bonus to all participants in all studies.

Table 3: We report expected loss $L_h(\pi)$ and expected cost $c(\pi)$ incurred (lower is better) in the last 10 trials by Prolific participants for each Algorithm and **bold** the variant with the lowest $L_h(\pi)$. We also consider different choices of λ , where $\lambda = 1.0$ corresponds to the cost-agnostic setting and $\lambda \neq 1.0$ corresponds to a cost-aware setting, where the choice of λ was selected according to our cost-aware workflow.

Algorithm	$L_h(\pi)$	$c(\pi)$	Algorithm	$L_h(\pi)$	$c(\pi)$
H-ONLY	0.68 ± 0.13	0	H-ONLY	0.51 ± 0.14	0
H-MODEL	0.50 ± 0.11	0.5	H-LLM	0.22 ± 0.14	0.1
H-CONSENSUS	0.32 ± 0.07	0.5	Population	0.33 ± 0.19	0.06 ± 0.01
Population	0.66 ± 0.08	0	Modiste-LinUCB ($\lambda = 1.0$)	0.25 ± 0.11	0.05 ± 0.02
Modiste-LinUCB ($\lambda = 1.0$)	0.22 ± 0.15	0.38 ± 0.06	Modiste-KNN ($\lambda = 1.0$)	0.3 ± 0.05	0.07 ± 0.02
Modiste-KNN ($\lambda = 1.0$)	0.1 ± 0.06	0.44 ± 0.07	Modiste-LinUCB ($\lambda = 0.95$)	0.35 ± 0.14	0.04 ± 0.01
Modiste-LinUCB ($\lambda = 0.85$)	0.5 ± 0.15	0.14 ± 0.07	Modiste-KNN ($\lambda = 0.75$)	0.3 ± 0.11	0.07 ± 0.02
Modiste-KNN ($\lambda = 0.75$)	0.14 ± 0.23	0.39 ± 0.06			

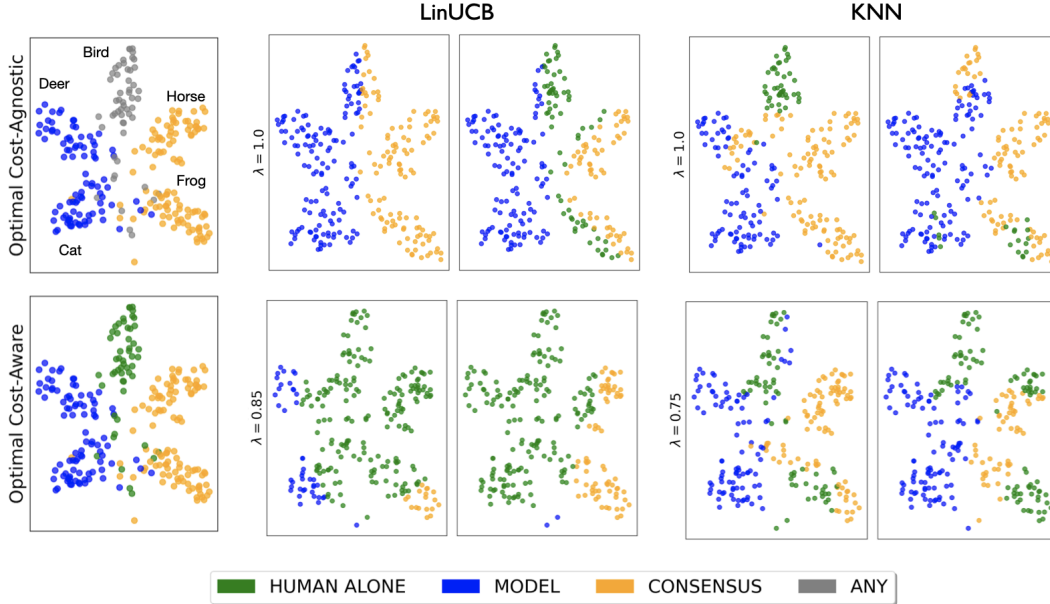


Figure 4: Snapshots of the learned decision support policies computed at the end of 100 interactions with randomly sampled users for CIFAR-3A. The forms of support are colored in t-SNE embedding space. In the cost-agnostic setting, both LinUCB and KNN generally identify the optimal form of support for a given input. Since the choice of support for images of Birds does not matter given the task set-up, we nicely find that when we introduce cost (i.e., when $\lambda \neq 1$), the learned policies favor the cheaper H-ONLY arm for images of Birds. All participant plots are included in Figure 12.

Trade-off parameter selection. For our cost-agnostic experiments, we let $\lambda = 1.0$ for each variant across all datasets. For our cost-aware experiments, we follow the strategies specified in the previous section to identify λ for each variant. We visualize this process in detail in Figure 9. For CIFAR-3A, the selected parameter values were $\lambda = 0.85$ for LinUCB and $\lambda = 0.75$ for KNN. For MMLU-2A, the selected parameter values were $\lambda = 0.95$ for LinUCB and $\lambda = 0.75$ for KNN.

Assessing personalized access

We recover the policies expected for CIFAR-3A. By design, the CIFAR-3A task compels “varying” profiles: Modiste’s forte. We find that Modiste learns to reconstruct near-optimal policies in both the standard and cost-aware settings, as depicted in Figure 4, for unseen users.

Modiste learns online to provide users with model predictions for two classes, with expert consensus for another two classes, and no support for the final class. This is reflected quantitatively in Table 3, where both Modiste variants, particularly KNN, have lower expected losses than any of the offline policies. Using our human-informed synthetic decision-makers, we also identify a choice of λ for each algorithm that modulates loss versus cost, which leads to a policy that uses the cheaper form of support (H-ONLY) more. However, the trade-off parameter affects the method differently, as the gap between the KNN variants is much smaller than that between the LinUCB variants.

We learn to provide LLM access selectively for MMLU-2A. Polymaths are rare; we observe no different in our

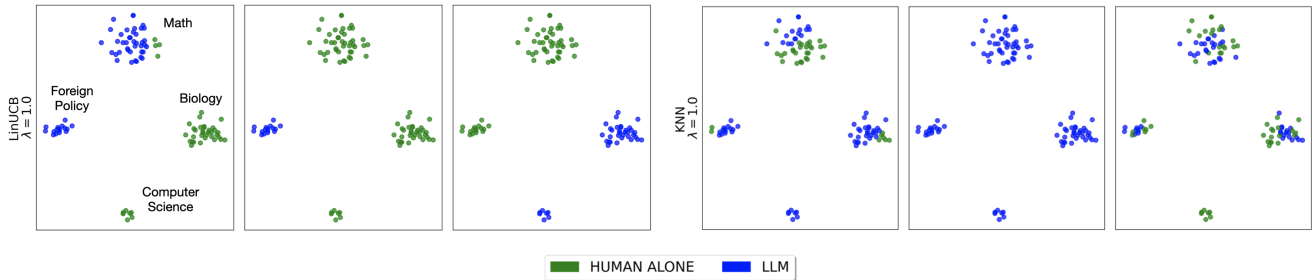


Figure 5: Snapshots of the learned decision support policies computed at the end of 60 interactions for MMLU-3A. The forms of support are colored in t-SNE embedding space. All six participants achieve $L_h(\pi) = 0.1875$ —comparable to the loss achieved by H-LLM—but exhibit distinct policies across input space. *Modiste* learns policies that capture each decision-maker’s strengths and weaknesses. All other participant plots are in Appendix Figure 11.

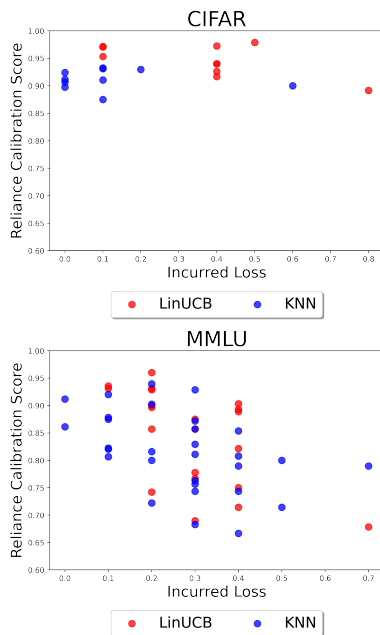


Figure 6: Relationship between a participant’s sensibility of reliance (measured as the proportion of times they correctly agreed or disagreed with the form of support’s prediction) and the loss incurred by the participant’s learned policy. In the MMLU task, *Modiste* performs best for participants who sensibly rely on the provided support. Reliance is computed over all trials (100 for CIFAR-3A, 60 for MMLU-2A), and loss is averaged over the final 10 timesteps.

Prolific data, as most participants struggle with at least one of the MMLU topics. As a result, *Modiste* learns that many individuals benefit from receiving the LLM as support, due in part to our task design (wherein the LLM excels at three of the four topics). In Figure 5, we see that *Modiste* personalizes support to decision-maker expertise, yielding policies that provide support on different topics for different decision-makers. Some users benefit from having the LLM all of the time (“strictly better” profile) while others can do without LLM for some topics. In Table 3, *Modiste* is not statistically different from the best baselines (H-LLM) in terms

of expected loss. Yet, we observe lower expected costs for both LinUCB and KNN in the cost-agnostic setting, and find similar results, as expected, in the cost-aware setting. This suggests that learning policies with *Modiste* has merit: participants who have no expertise can expect to receive support from the LLM, and those who are proficient in one topic, but not in another, can expect to see the LLM in only cases beyond their expertise. While $L_h(\pi)$ of the *Modiste* variants are similar to that of the Population baseline in Table 3, the variance is significantly smaller—particularly with KNN—underscoring the benefits of personalization.

Discussion

Our human subject experiments validate trends observed in the computational experiments in both the cost-agnostic and cost-aware settings, demonstrating that *Modiste* can be used to learn decision support policies online. We find that learning personalized policies leads to performance and cost benefits when encountering users with “varying” expertise profiles, and recovers fixed policies for participants with “strictly better” profiles in the cost-agnostic setting. While our human-informed synthetic decision-makers permit us to pick a suitable λ for unseen study participants, future work modeling human idiosyncrasies (Steyvers and Kumar 2022) explicitly in synthetic decision-makers may bolster the effectiveness of personalization.

Participants’ reliance is one such factor. We define a metric for “reliance sensibility,” as the proportion of trials where the participant agreed with the support when correct and responded differently when the support was incorrect, out of all trials where the participant received support. The higher the proportion, the more “sensible” a participant’s degree of reliance on the provided support is, relative to what would be most beneficial for decision outcomes.⁴ We plot the performance of the learned policy (i.e., incurred loss) against a participant’s reliance sensibility in Figure 6. In CIFAR-3A, participants largely had calibrated reliance because, by

⁴Note that we cannot directly deduce whether, or to what degree, an individual participant relied on the form of support when presented - since we do not have access to what an individual would have said without support; alternative reliance inference schemes like (Tejeda et al. 2022) could be considered in future work.

design, there was a signal for when to rely on each form of support. However, in the MMLU setting, we observe a variety of reliance behavior spanning over- and under-reliance, as we would expect in-the-wild (Zerilli, Bhatt, and Weller 2022). We also find a negative correlation between expected loss and reliance (Pearson r correlation = -0.47 and -0.59 for KNN and LinUCB, respectively), indicating that `Modiste` was less effective for participants who did not appropriately rely on support. At present, `Modiste` only considers expertise explicitly when personalizing policies, yet these data underscore the importance of understanding when individual decision-makers may over-rely on potentially fallible support (Bussone, Stumpf, and O’Sullivan 2015). We explore practical considerations of personalized policies next.

Practical Considerations

An important concern of `Modiste` stems from our encouragement for individuals to *disuse* decision support. In particular, as machine learning models are increasingly used as a form of decision-support (Lai et al. 2023), our approach to learning a decision support policy promotes the disuse of models in favor of human judgment and agency. Automating access to model outputs may disadvantage individuals whose behavior (i.e., observed decisions) is misaligned with their values and may be used by organizations to prevent access to model outputs in a “big brother” sense (Zuboff 2023). We acknowledge that future work may need to justify to decision-makers when they are barred from accessing the model. This may lead to important intersections with the legal and policy communities. Instead of fully restricting access, less strict forms of disuse can be used to friction the decision-maker’s experience with a model, while having the same effect as barring access: examples include hiding the model output, which can be clicked on to appear (Buçinca, Malaya, and Gajos 2021), or displaying model confidence only for uncertain inputs (Antoran et al. 2020).

Additionally, since personalization inherently requires the use of participatory data (James et al. 2023), there will likely need to be explicit consent for the data to be used in learning decision support policies. Though our personalized policies make no assumptions about access to data from individuals a priori when learning a decision support policy, we use data collected from a like population, but we imagine that similar approaches can be used to design policies with offline user data (Charusaie et al. 2022; Buçinca et al. 2024). There may be unintended, negative impacts of collecting such data as organizations can use this data to implement nefarious decision support policies, whereby members are manipulated into using decision support, or to track user behavior. While we hope that personalized decision support policies encourage the thoughtful use of decision support, we caution against the ways that adverse actors can leverage these tools to privilege a select few, who in turn reap the benefits of personalized access to decision support tools (Gabriel et al. 2024).

Finally, the settings in which our tool, `Modiste`, was evaluated targeted English-language-speaking crowdworkers. The ecological validity (Zerilli, Bhatt, and Weller 2022) of our results may not hold for other groups, whose experiences, values, and preferences with respect to the use of machine

learning models in decision-making may differ. While we did receive requisite approval to learn personalized policies on human subjects from our institution’s IRB, we hope that future work can cast a wider net for running experiments on groups of differing positionality (Kirk et al. 2024). Relatedly, our human subject experiments focused on two tasks (CIFAR and MMLU), which are relatively low-stakes decisions. We encourage future work to study similar problem formulations for personalized support in higher-stakes settings. We sincerely hope that decision support policies become a pervasive mechanism for empowering individuals to take control when models are provided to them.

Conclusion

A decision support policy captures when and which form of support should be provided to improve a decision-maker’s performance. The selective use of AI-based decision support helps instantiate the “appropriate use” clauses in emerging regulation (Biden 2023), as we only provide AI assistance to decision-makers as and when it is beneficial to them. We introduce `Modiste`, an interactive tool for learning a decision support policy for each decision-maker using contextual bandits. To the best of our knowledge, we are the first to learn and validate such a policy online for unseen decision-makers. Within our `Modiste` interface, we instantiate two variants of Algorithm 1 using existing stochastic contextual bandit tools, namely LinUCB and online KNN. We consider both cost-agnostic and cost-aware policies for providing decision-makers with access to decision support. Our computational and human subject experiments highlight the importance—and feasibility—of personalizing decision support policies for individual decision-makers. Our human subject experiments are encouraging, demonstrating that we can learn decision support policies in remarkably few iterations and tease apart differences in decision-makers’ need for support. While encouraging rich cross-talk between domain experts and practitioners, future work integrating `Modiste` into existing decision-making workflows would pave a route towards responsible use of AI as decision support.

While we obtain promising results with `Modiste`, we acknowledge that we only consider the classification setting here where we get immediate feedback (e.g., we can calculate the loss to update π). We imagine that extending to a delayed feedback setting or to a different cognitive task (e.g., planning or perception) would prove fruitful. As with most online learning algorithms, selecting a suitable explore-exploit trade-off (a la Table 6) can prove challenging, though we find that our learned policy is preferable to the fixed policies used in practice at the moment. Though `Modiste` is promising, we note that significant issues can arise when decision-makers blindly rely on decision support (Buçinca et al. 2020), especially when the support is erroneous or ineffective; such over-reliance requires careful attention to prevent. Second, our problem definition hinges on domain experts defining the available forms of support (i.e., we need a clearly defined \mathcal{A} to use `Modiste`). In practice, this may prove difficult, as one may not know how to define specific forms of support or decision-makers may have access to varying support sets due to regulatory or organizational reasons. Nonetheless,

the promise of using ML models as decision support rests on our ability to provide the right form of support to the right decision-maker at the right time: *Modiste* takes a step towards realizing personalized access to decision support.

Acknowledgements

UB acknowledges support from DeepMind and the Leverhulme Trust via the Leverhulme Centre for the Future of Intelligence (CFI). AW acknowledges support from a Turing AI Fellowship under grant EP/V025279/1, EPSRC grants EP/V056522/1 and EP/V056883/1, and the Leverhulme Trust via CFI. KMC acknowledges support from a Marshall Scholarship and the Cambridge Trust. PK acknowledges support from The Alan Turing Institute. AT acknowledges support from the National Science Foundation grants IIS1705121, IIS1838017, IIS2046613, IIS2112471, an Amazon Web Services Award, a Facebook Faculty Research Award, funding from Booz Allen Hamilton Inc., and a Block Center Grant. Any opinions, findings and conclusions or recommendations expressed in this material are those of the author(s) and do not necessarily reflect the views of any of these funding agencies. We thank the Prolific participants who took part in our studies, as well as our Cambridge-based volunteer pilot participants. We thank Alan Liu and Kartik Chandra for their invaluable input on designing our web-based server.

References

2023. European Parliament, “Amendments adopted by the European Parliament on 14 June 2023 on the proposal for a regulation of the European Parliament and of the Council on laying down harmonised rules on artificial intelligence (Artificial Intelligence Act) and amending certain Union legislative acts” (COM(2021)0206 – C9-0146/2021 – 2021/0106(COD), European Parliament, 2023).
- Amodei, D.; Olah, C.; Steinhardt, J.; Christiano, P.; Schulman, J.; and Mané, D. 2016. Concrete problems in AI safety. *arXiv preprint arXiv:1606.06565*.
- Antoran, J.; Bhatt, U.; Adel, T.; Weller, A.; and Hernández-Lobato, J. M. 2020. Getting a CLUE: A Method for Explaining Uncertainty Estimates. In *International Conference on Learning Representations*.
- Arbiser, Z. K.; Folpe, A. L.; and Weiss, S. W. 2001. Consultative (expert) second opinions in soft tissue pathology: analysis of problem-prone diagnostic situations. *American journal of clinical pathology*, 116(4): 473–476.
- Augustin, A.; Venanzi, M.; Rogers, A.; and Jennings, N. R. 2017. Bayesian Aggregation of Categorical Distributions with Applications in Crowdsourcing. In *IJCAI*, 1411–1417.
- Babbar, V.; Bhatt, U.; and Weller, A. 2022. On the Utility of Prediction Sets in Human-AI Teams. In Raedt, L. D., ed., *Proceedings of the Thirty-First International Joint Conference on Artificial Intelligence, IJCAI-22*, 2457–2463. International Joint Conferences on Artificial Intelligence Organization. Main Track.
- Bakker, M. A.; Tu, D. P.; Gummadi, K. P.; Pentland, A. S.; Varshney, K. R.; and Weller, A. 2021. Beyond reasonable doubt: Improving fairness in budget-constrained decision making using confidence thresholds. In *Proceedings of the 2021 AAAI/ACM Conference on AI, Ethics, and Society*, 346–356.
- Bansal, G.; Nushi, B.; Kamar, E.; Horvitz, E.; and Weld, D. S. 2021a. Is the most accurate AI the best teammate? optimizing AI for teamwork. In *Proceedings of the AAAI Conference on Artificial Intelligence*, volume 35, 11405–11414.
- Bansal, G.; Wu, T.; Zhou, J.; Fok, R.; Nushi, B.; Kamar, E.; Ribeiro, M. T.; and Weld, D. 2021b. Does the whole exceed its parts? The effect of AI explanations on complementary team performance. In *Proceedings of the 2021 CHI Conference on Human Factors in Computing Systems*, 1–16.
- Barabas, C. 2022. Refusal in Data Ethics: Re-Imagining the Code Beneath the Code of Computation in the Carceral State. *Engaging Science, Technology, and Society*, 8(2): 35–57.
- Bastani, H.; Bastani, O.; and Sinchaisri, P. 2022. Improving Human Decision-Making with Machine Learning. In *Academy of Management Proceedings*, volume 2022, 17725. Academy of Management Briarcliff Manor, NY 10510.
- Bastani, H.; and Bayati, M. 2020. Online decision making with high-dimensional covariates. *Operations Research*, 68(1): 276–294.
- Bates, S.; Angelopoulos, A.; Lei, L.; Malik, J.; and Jordan, M. 2021. Distribution-free, risk-controlling prediction sets. *Journal of the ACM (JACM)*, 68(6): 1–34.
- Battleday, R. M.; Peterson, J. C.; and Griffiths, T. L. 2020. Capturing human categorization of natural images by combining deep networks and cognitive models. *Nature communications*, 11(1): 1–14.
- Beyer, L.; Hénaff, O. J.; Kolesnikov, A.; Zhai, X.; and van den Oord, A. 2020. Are we done with ImageNet? *CoRR*, abs/2006.07159.
- Bhatt, U.; Antorán, J.; Zhang, Y.; Liao, Q. V.; Sattigeri, P.; Fogliato, R.; Melançon, G.; Krishnan, R.; Stanley, J.; Tickoo, O.; Nachman, L.; Chunara, R.; Srikumar, M.; Weller, A.; and Xiang, A. 2021. Uncertainty as a Form of Transparency: Measuring, Communicating, and Using Uncertainty. In *Proceedings of the 2021 AAAI/ACM Conference on AI, Ethics, and Society*, 401–413. New York, NY, USA. ISBN 9781450384735.
- Biden, J. R. 2023. *Executive Order 14110, Executive Order on the Safe, Secure, and Trustworthy Development and Use of Artificial Intelligence*. The White House.
- Bommasani, R.; Hudson, D. A.; Adeli, E.; Altman, R. B.; Arora, S.; von Arx, S.; Bernstein, M. S.; Bohg, J.; Bosselut, A.; Brunskill, E.; Brynjolfsson, E.; Buch, S.; Card, D.; Castellon, R.; Chatterji, N. S.; Chen, A. S.; Creel, K.; Davis, J. Q.; Demszky, D.; Donahue, C.; Doumbouya, M.; Durmus, E.; Ermon, S.; Etchemendy, J.; Ethayarajh, K.; Fei-Fei, L.; Finn, C.; Gale, T.; Gillespie, L.; Goel, K.; Goodman, N. D.; Grossman, S.; Guha, N.; Hashimoto, T.; Henderson, P.; Hewitt, J.; Ho, D. E.; Hong, J.; Hsu, K.; Huang, J.; Icard, T.; Jain, S.; Jurafsky, D.; Kalluri, P.; Karamcheti, S.; Keeling, G.; Khani, F.; Khattab, O.; Koh, P. W.; Krass, M. S.; Krishna, R.; Kudithipudi, R.; and et al. 2021. On the Opportunities and Risks of Foundation Models. *CoRR*, abs/2108.07258.
- Bondi, E.; Koster, R.; Sheahan, H.; Chadwick, M.; Bachrach, Y.; Cemgil, T.; Paquet, U.; and Dvijotham, K. 2022. Role of

- Human-AI Interaction in Selective Prediction. *Proceedings of the AAAI Conference on Artificial Intelligence*.
- Bordt, S.; and Von Luxburg, U. 2022. A Bandit Model for Human-Machine Decision Making with Private Information and Opacity. In *International Conference on Artificial Intelligence and Statistics*, 7300–7319. PMLR.
- Briggs, G. M.; Flynn, P. A.; Worthington, M.; Rennie, I.; and McKinstry, C. 2008. The role of specialist neuroradiology second opinion reporting: is there added value? *Clinical radiology*, 63(7): 791–795.
- Brundage, M.; Avin, S.; Clark, J.; Toner, H.; Eckersley, P.; Garfinkel, B.; Dafoe, A.; Scharre, P.; Zeitzoff, T.; Filar, B.; et al. 2018. The malicious use of artificial intelligence: Forecasting, prevention, and mitigation. *arXiv preprint arXiv:1802.07228*.
- Buçinca, Z.; Lin, P.; Gajos, K. Z.; and Glassman, E. L. 2020. Proxy tasks and subjective measures can be misleading in evaluating explainable AI systems. In *Proceedings of the 25th International Conference on Intelligent User Interfaces*, 454–464.
- Buçinca, Z.; Malaya, M. B.; and Gajos, K. Z. 2021. To trust or to think: cognitive forcing functions can reduce overreliance on AI in AI-assisted decision-making. *Proceedings of the ACM on Human-Computer Interaction*, 5(CSCW1): 1–21.
- Buçinca, Z.; Swaroop, S.; Paluch, A. E.; Murphy, S. A.; and Gajos, K. Z. 2024. Towards Optimizing Human-Centric Objectives in AI-Assisted Decision-Making With Offline Reinforcement Learning. *arXiv preprint arXiv:2403.05911*.
- Bussone, A.; Stumpf, S.; and O’Sullivan, D. 2015. The role of explanations on trust and reliance in clinical decision support systems. In *2015 international conference on healthcare informatics*, 160–169. IEEE.
- Camburu, O.-M.; Rocktäschel, T.; Lukasiewicz, T.; and Blunsom, P. 2018. e-snli: Natural language inference with natural language explanations. *Advances in Neural Information Processing Systems*, 31.
- Charusaie, M.-A.; Mozannar, H.; Sontag, D.; and Samadi, S. 2022. Sample Efficient Learning of Predictors that Complement Humans. In *International Conference on Machine Learning*, 2972–3005. PMLR.
- Chen, V.; Li, J.; Kim, J. S.; Plumb, G.; and Talwalkar, A. 2022. Interpretable machine learning: Moving from mythos to diagnostics. *Queue*, 19(6): 28–56.
- Chen, V.; Liao, Q. V.; Wortman Vaughan, J.; and Bansal, G. 2023. Understanding the role of human intuition on reliance in human-AI decision-making with explanations. *Proceedings of the ACM on Human-Computer Interaction*, 7(CSCW2): 1–32.
- Chow, C.-K. 1957. An optimum character recognition system using decision functions. *IRE Transactions on Electronic Computers*, (4): 247–254.
- Collins, K. M.; Barker, M.; Zarlenga, M. E.; Raman, N.; Bhatt, U.; Jamnik, M.; Sucholutsky, I.; Weller, A.; and Dvijotham, K. 2023a. Human Uncertainty in Concept-Based AI Systems. [arXiv:2303.12872](https://arxiv.org/abs/2303.12872).
- Collins, K. M.; Bhatt, U.; and Weller, A. 2022. Eliciting and Learning with Soft Labels from Every Annotator. In *Proceedings of the AAAI Conference on Human Computation and Crowdsourcing (HCOMP)*, volume 10.
- Collins, K. M.; Jiang, A. Q.; Frieder, S.; Wong, L.; Zilka, M.; Bhatt, U.; Lukasiewicz, T.; Wu, Y.; Tenenbaum, J. B.; Hart, W.; et al. 2023b. Evaluating language models for mathematics through interactions. *arXiv preprint arXiv:2306.01694*.
- Cortes, C.; DeSalvo, G.; Gentile, C.; Mohri, M.; and Yang, S. 2018. Online learning with abstention. In *International conference on machine learning*, 1059–1067. PMLR.
- Cortes, C.; DeSalvo, G.; and Mohri, M. 2016. Learning with rejection. In *International Conference on Algorithmic Learning Theory*, 67–82. Springer.
- Dawid, A. P.; and Skene, A. M. 1979. Maximum likelihood estimation of observer error-rates using the EM algorithm. *Journal of the Royal Statistical Society: Series C (Applied Statistics)*, 28(1): 20–28.
- De-Arteaga, M.; Dubrawski, A.; and Chouldechova, A. 2018. Learning under selective labels in the presence of expert consistency. *arXiv preprint arXiv:1807.00905*.
- Ehsan, U.; Harrison, B.; Chan, L.; and Riedl, M. O. 2018. Rationalization: A neural machine translation approach to generating natural language explanations. In *Proceedings of the 2018 AAAI/ACM Conference on AI, Ethics, and Society*, 81–87.
- Erramilli, M. K. 1996. Nationality and subsidiary ownership patterns in multinational corporations. *Journal of International Business Studies*, 27: 225–248.
- Gabriel, I.; Manzini, A.; Keeling, G.; Hendricks, L. A.; Rieser, V.; Iqbal, H.; Tomašev, N.; Ktena, I.; Kenton, Z.; Rodriguez, M.; et al. 2024. The Ethics of Advanced AI Assistants. *arXiv preprint arXiv:2404.16244*.
- Gao, R.; Saar-Tsechansky, M.; De-Arteaga, M.; Han, L.; Lee, M. K.; and Lease, M. 2021. Human-AI Collaboration with Bandit Feedback. In *Proceedings of the Thirtieth International Joint Conference on Artificial Intelligence, IJCAI-21*, 1722–1728. International Joint Conferences on Artificial Intelligence Organization.
- Gao, R.; Saar-Tsechansky, M.; De-Arteaga, M.; Han, L.; Sun, W.; Lee, M. K.; and Lease, M. 2023. Learning Complementary Policies for Human-AI Teams. *arXiv preprint arXiv:2302.02944*.
- Geifman, Y.; and El-Yaniv, R. 2017. Selective classification for deep neural networks. *Advances in neural information processing systems*, 30.
- Gordon, E.; and Mugar, G. 2020. *Meaningful inefficiencies: designing for public value in an age of digital expediency*. New York, NY: Oxford University Press. ISBN 978-0-19-087017-1 978-0-19-087016-4 978-0-19-087015-7.
- Gordon, M. L.; Lam, M. S.; Park, J. S.; Patel, K.; Hancock, J.; Hashimoto, T.; and Bernstein, M. S. 2022. Jury learning: Integrating dissenting voices into machine learning models. In *CHI Conference on Human Factors in Computing Systems*, 1–19.

- Gordon, M. L.; Zhou, K.; Patel, K.; Hashimoto, T.; and Bernstein, M. S. 2021. The disagreement deconvolution: Bringing machine learning performance metrics in line with reality. In *Proceedings of the 2021 CHI Conference on Human Factors in Computing Systems*, 1–14.
- Green, B.; and Chen, Y. 2019. The principles and limits of algorithm-in-the-loop decision making. *Proceedings of the ACM on Human-Computer Interaction*, 3(CSCW): 1–24.
- Guan, M.; and Jiang, H. 2018. Nonparametric stochastic contextual bandits. In *Proceedings of the AAAI Conference on Artificial Intelligence*, volume 32.
- Harrell, F. E.; Califf, R. M.; Pryor, D. B.; Lee, K. L.; and Rosati, R. A. 1982. Evaluating the yield of medical tests. *Jama*, 247(18): 2543–2546.
- He, K.; Zhang, X.; Ren, S.; and Sun, J. 2016. Deep residual learning for image recognition. In *CVPR*, 770–778.
- Hemmer, P.; Schellhammer, S.; Vössing, M.; Jakubik, J.; and Satzger, G. 2022. Forming Effective Human-AI Teams: Building Machine Learning Models that Complement the Capabilities of Multiple Experts. In *Proceedings of the Thirtieth International Conference on International Joint Conferences on Artificial Intelligence*.
- Hemmer, P.; Westphal, M.; Schemmer, M.; Vetter, S.; Vössing, M.; and Satzger, G. 2023. Human-AI Collaboration: The Effect of AI Delegation on Human Task Performance and Task Satisfaction. In *Proceedings of the 28th International Conference on Intelligent User Interfaces*, 453–463.
- Hendrycks, D.; Burns, C.; Basart, S.; Zou, A.; Mazeika, M.; Song, D.; and Steinhardt, J. 2020. Measuring Massive Multi-task Language Understanding. In *International Conference on Learning Representations*.
- Hullman, J.; Qiao, X.; Correll, M.; Kale, A.; and Kay, M. 2018. In pursuit of error: A survey of uncertainty visualization evaluation. *IEEE transactions on visualization and computer graphics*, 25(1): 903–913.
- James, H.; Nagpal, C.; Heller, K. A.; and Ustun, B. 2023. Participatory Personalization in Classification. In *Thirty-seventh Conference on Neural Information Processing Systems*.
- Jeyakumar, J. V.; Noor, J.; Cheng, Y.-H.; Garcia, L.; and Srivastava, M. 2020. How Can I Explain This to You? An Empirical Study of Deep Neural Network Explanation Methods. *Advances in Neural Information Processing Systems*, 33.
- Kahn Jr, C. E. 1994. Artificial intelligence in radiology: decision support systems. *Radiographics*, 14(4): 849–861.
- Kalis, A.; Kaiser, S.; and Mojzisch, A. 2013. Why we should talk about option generation in decision-making research. *Frontiers in psychology*, 4: 555.
- Keen, P. G. 1980. Decision support systems: a research perspective. In *Decision support systems: Issues and challenges: Proceedings of an international task force meeting*, 23–44.
- Keswani, V.; Lease, M.; and Kenthapadi, K. 2021. Towards unbiased and accurate deferral to multiple experts. In *Proceedings of the 2021 AAAI/ACM Conference on AI, Ethics, and Society*, 154–165.
- Kim, B.; Rudin, C.; and Shah, J. A. 2014. The bayesian case model: A generative approach for case-based reasoning and prototype classification. In *Advances in neural information processing systems*, 1952–1960.
- Kirk, H. R.; Whitefield, A.; Röttger, P.; Bean, A.; Margatina, K.; Ciro, J.; Mosquera, R.; Bartolo, M.; Williams, A.; He, H.; et al. 2024. The PRISM Alignment Project: What Participatory, Representative and Individualised Human Feedback Reveals About the Subjective and Multicultural Alignment of Large Language Models. *arXiv preprint arXiv:2404.16019*.
- Krizhevsky, A. 2009. Learning Multiple Layers of Features from Tiny Images. *Master's thesis, University of Toronto*.
- Lai, V.; Carton, S.; Bhatnagar, R.; Liao, Q. V.; Zhang, Y.; and Tan, C. 2022. Human-AI Collaboration via Conditional Delegation: A Case Study of Content Moderation. In *CHI Conference on Human Factors in Computing Systems*, 1–18.
- Lai, V.; Chen, C.; Smith-Renner, A.; Liao, Q. V.; and Tan, C. 2023. Towards a Science of Human-AI Decision Making: An Overview of Design Space in Empirical Human-Subject Studies. In *Proceedings of the 2023 ACM Conference on Fairness, Accountability, and Transparency*, 1369–1385.
- Laidlaw, C.; and Russell, S. 2021. Uncertain Decisions Facilitate Better Preference Learning. *Advances in Neural Information Processing Systems*, 34: 15070–15083.
- Lee, M.; Srivastava, M.; Hardy, A.; Thickstun, J.; Durmus, E.; Paranjape, A.; Gerard-Ursin, I.; Li, X. L.; Ladhak, F.; Rong, F.; Wang, R. E.; Kwon, M.; Park, J. S.; Cao, H.; Lee, T.; Bommasani, R.; Bernstein, M. S.; and Liang, P. 2023. Evaluating Human-Language Model Interaction. *Transactions on Machine Learning Research*.
- Li, L.; Chu, W.; Langford, J.; and Schapire, R. E. 2010. A contextual-bandit approach to personalized news article recommendation. In *Proceedings of the 19th international conference on World wide web*, 661–670.
- Lichtenstein, S.; Fischhoff, B.; and Phillips, L. D. 1977. Calibration of probabilities: The state of the art. *Decision making and change in human affairs*, 275–324.
- Ma, S.; Lei, Y.; Wang, X.; Zheng, C.; Shi, C.; Yin, M.; and Ma, X. 2023. Who should i trust: Ai or myself? leveraging human and ai correctness likelihood to promote appropriate trust in ai-assisted decision-making. In *Proceedings of the 2023 CHI Conference on Human Factors in Computing Systems*, 1–19.
- Madras, D.; Pitassi, T.; and Zemel, R. 2018. Predict responsibly: improving fairness and accuracy by learning to defer. *Advances in Neural Information Processing Systems*, 31.
- Mimra, W.; Rasch, A.; and Waibel, C. 2016. Second opinions in markets for expert services: Experimental evidence. *Journal of Economic Behavior & Organization*, 131: 106–125.
- Mozannar, H.; Bansal, G.; Fourney, A.; and Horvitz, E. 2022. Reading Between the Lines: Modeling User Behavior and Costs in AI-Assisted Programming. *arXiv preprint arXiv:2210.14306*.
- Mozannar, H.; Lee, J.; Wei, D.; Sattigeri, P.; Das, S.; and Sontag, D. 2023. Effective Human-AI Teams via Learned

- Natural Language Rules and Onboarding. In Oh, A.; Naumann, T.; Globerson, A.; Saenko, K.; Hardt, M.; and Levine, S., eds., *Advances in Neural Information Processing Systems*, volume 36, 30466–30498. Curran Associates, Inc.
- Mozannar, H.; Satyanarayan, A.; and Sontag, D. 2022. Teaching Humans When To Defer to a Classifier via Exemplars. In *Proceedings of the AAAI Conference on Artificial Intelligence*, volume 36, 5323–5331.
- Mozannar, H.; and Sontag, D. 2020. Consistent estimators for learning to defer to an expert. In *International Conference on Machine Learning*, 7076–7087. PMLR.
- Mylonakis, E.; Paliou, M.; Greenbough, T. C.; Flanigan, T. P.; Letvin, N. L.; and Rich, J. D. 2000. Report of a false-positive HIV test result and the potential use of additional tests in establishing HIV serostatus. *Archives of internal medicine*, 160(15): 2386–2388.
- Nakano, R.; Hilton, J.; Balaji, S.; Wu, J.; Ouyang, L.; Kim, C.; Hesse, C.; Jain, S.; Kosaraju, V.; Saunders, W.; Jiang, X.; Cobbe, K.; Eloundou, T.; Krueger, G.; Button, K.; Knight, M.; Chess, B.; and Schulman, J. 2021. WebGPT: Browser-assisted question-answering with human feedback. *CoRR*, abs/2112.09332.
- Noti, G.; and Chen, Y. 2023. Learning when to advise human decision makers. In *Proceedings of the Thirty-Second International Joint Conference on Artificial Intelligence*, 3038–3048.
- O’Hagan, A.; Buck, C. E.; Daneshkhah, A.; Eiser, J. R.; Garthwaite, P. H.; Jenkinson, D. J.; Oakley, J. E.; and Rakow, T. 2006. *Uncertain Judgements: Eliciting Expert Probabilities*. Chichester: John Wiley.
- Okati, N.; De, A.; and Rodriguez, M. 2021. Differentiable learning under triage. *Advances in Neural Information Processing Systems*, 34: 9140–9151.
- Ouyang, L.; Wu, J.; Jiang, X.; Almeida, D.; Wainwright, C. L.; Mishkin, P.; Zhang, C.; Agarwal, S.; Slama, K.; Ray, A.; Schulman, J.; Hilton, J.; Kelton, F.; Miller, L.; Simens, M.; Askell, A.; Welinder, P.; Christiano, P.; Leike, J.; and Lowe, R. 2022. Training language models to follow instructions with human feedback.
- Palan, S.; and Schitter, C. 2018. Prolific. ac—A subject pool for online experiments. *Journal of Behavioral and Experimental Finance*, 17: 22–27.
- Peterson, J. C.; Battleday, R. M.; Griffiths, T. L.; and Ruskovskiy, O. 2019. Human uncertainty makes classification more robust. In *Proceedings of the IEEE/CVF International Conference on Computer Vision*, 9617–9626.
- Phillips-Wren, G. 2012. AI tools in decision making support systems: a review. *International Journal on Artificial Intelligence Tools*, 21(02): 1240005.
- Ribeiro, M. T.; Singh, S.; and Guestrin, C. 2016. ” Why should i trust you?” Explaining the predictions of any classifier. In *Proceedings of the 22nd ACM SIGKDD international conference on knowledge discovery and data mining*, 1135–1144.
- Roda, C. E. 2011. *Human attention and its implications for human-computer interaction*. Cambridge University Press.
- Scheife, R. T.; Hines, L. E.; Boyce, R. D.; Chung, S. P.; Momper, J. D.; Sommer, C. D.; Abernethy, D. R.; Horn, J. R.; Sklar, S. J.; Wong, S. K.; et al. 2015. Consensus recommendations for systematic evaluation of drug–drug interaction evidence for clinical decision support. *Drug safety*, 38(2): 197–206.
- Schvaneveldt, R. W.; Durso, F. T.; Goldsmith, T. E.; Breen, T. J.; Cooke, N. M.; Tucker, R. G.; and De Maio, J. C. 1985. Measuring the structure of expertise. *International journal of man-machine studies*, 23(6): 699–728.
- Seger, C. A.; and Peterson, E. J. 2013. Categorization= decision making+ generalization. *Neuroscience & Biobehavioral Reviews*, 37(7): 1187–1200.
- Spiegelhalter, D. 2017. Risk and Uncertainty Communication. 4(1): 31–60.
- Steyvers, M.; and Kumar, A. 2022. Three Challenges for AI-Assisted Decision-Making.
- Straitouri, E.; Wang, L.; Okati, N.; and Rodriguez, M. G. 2022. Provably improving expert predictions with conformal prediction. *arXiv preprint arXiv:2201.12006*.
- Sutton, R. S.; and Barto, A. G. 2018. *Reinforcement learning: An introduction*.
- Swaroop, S.; Buçinca, Z.; Gajos, K. Z.; and Doshi-Velez, F. 2024. Accuracy-Time Tradeoffs in AI-Assisted Decision Making under Time Pressure. In *Proceedings of the 29th International Conference on Intelligent User Interfaces*, 138–154.
- Tejeda, H.; Kumar, A.; Smyth, P.; and Steyvers, M. 2022. AI-assisted decision-making: A cognitive modeling approach to infer latent reliance strategies. *Computational Brain & Behavior*, 1–18.
- Tekin, C.; and Turğay, E. 2018. Multi-objective contextual multi-armed bandit with a dominant objective. *IEEE Transactions on Signal Processing*, 66(14): 3799–3813.
- Turgay, E.; Oner, D.; and Tekin, C. 2018. Multi-objective contextual bandit problem with similarity information. In *International Conference on Artificial Intelligence and Statistics*, 1673–1681. PMLR.
- Tversky, A.; and Kahneman, D. 1996. On the reality of cognitive illusions. *Psychological Review*, 103(3): 582–591.
- Uma, A.; Almanea, D.; and Poesio, M. 2022. Scaling and Disagreements: Bias, Noise, and Ambiguity. *Frontiers in Artificial Intelligence*, 5.
- Uma, A.; Fornaciari, T.; Hovy, D.; Paun, S.; Plank, B.; and Poesio, M. 2020. A Case for Soft Loss Functions. *Proceedings of the AAAI Conference on Human Computation and Crowdsourcing*, 8(1): 173–177.
- Ustun, B.; Spangher, A.; and Liu, Y. 2019. Actionable recourse in linear classification. In *Proceedings of the Conference on Fairness, Accountability, and Transparency*, 10–19.
- Vovk, V. 1998. A game of prediction with expert advice. *Journal of Computer and System Sciences*, 56(2): 153–173.
- Vovk, V.; Gammerman, A.; and Shafer, G. 2005. *Algorithmic Learning in a Random World*. Springer.

- Wei, J.; Zhu, Z.; Cheng, H.; Liu, T.; Niu, G.; and Liu, Y. 2022. Learning with Noisy Labels Revisited: A Study Using Real-World Human Annotations. In *International Conference on Learning Representations*.
- Whitehill, J.; Wu, T.-f.; Bergsma, J.; Movellan, J.; and Ruolo, P. 2009. Whose vote should count more: Optimal integration of labels from labelers of unknown expertise. *Advances in neural information processing systems*, 22.
- Wilder, B.; Horvitz, E.; and Kamar, E. 2021. Learning to complement humans. In *Proceedings of the Twenty-Ninth International Conference on International Joint Conferences on Artificial Intelligence*, 1526–1533.
- Wolczynski, N.; Saar-Tsechansky, M.; and Wang, T. 2022. Learning to Advise Humans By Leveraging Algorithm Discretion. *arXiv preprint arXiv:2210.12849*.
- Yang, S.; Nachum, O.; Du, Y.; Wei, J.; Abbeel, P.; and Schuurmans, D. 2023. Foundation Models for Decision Making: Problems, Methods, and Opportunities. *arXiv preprint arXiv:2303.04129*.
- Zerilli, J.; Bhatt, U.; and Weller, A. 2022. How transparency modulates trust in artificial intelligence. *Patterns*, 100455.
- Zhang, Y.; Liao, Q. V.; and Bellamy, R. K. 2020. Effect of confidence and explanation on accuracy and trust calibration in AI-assisted decision making. In *Proceedings of the 2020 conference on fairness, accountability, and transparency*, 295–305.
- Zuboff, S. 2023. The age of surveillance capitalism. In *Social theory re-wired*, 203–213. Routledge.

Appendix

We provide details on decision support policies, additional computational experiments with `Modiste`, and extensive information on our human subject experiments with `Modiste`.

Comparison Against Prior Work

Most papers on human-AI collaboration have considered clever ways of abstaining from prediction on specific inputs (Cortes, DeSalvo, and Mohri 2016; Cortes et al. 2018), learning deferral functions based on multiple experts (Vovk 1998; Keswani, Lease, and Kenthapadi 2021), or teaching decision-makers when to rely (Mozannar, Satyanarayan, and Sontag 2022). There are also a number of papers from the HCI literature (see survey by (Lai et al. 2023)) that evaluate the two-action setting of our formulation using a *static* policy (e.g., always showing the ML model prediction or always showing some form of explanation).

To clarify how our set-up and assumptions differ from prior work, we overview work that we believe could be considered most similar to ours. We decompose our comparisons along a few dimensions: **Decision-support set-up:** Does the human make the final decision, or is it a different set-up? **Assumptions about decision-maker information:** What does prior work assume about access to a decision-maker when learning a policy? **Evaluation:** Does prior work simulate humans? Does prior work run user studies?

Mozannar and Sontag (2020) and Hemmer et al. (2023):

- **Decision-support set-up:** This work’s set-up can be considered a two-action setting of our formulation, where $\mathcal{A} = \{\text{DEFER}, \text{MODEL}\}$. Extending the work of Madras, Pitassi, and Zemel (2018), this work proposes the learning to defer paradigm, where the decision-maker may not always make a final decision (i.e., sometimes the decision is deferred entirely to an algorithmic-based system). In our set-up, deferring to a `MODEL` is equivalent to always adhering to a label-based form of support. The human is always the final decision-maker in our work, which is representative of many decision-making set-ups in practice (Lai et al. 2022), but not captured in this line of prior work.
- **Assumptions about decision-maker information:** This work assumes oracle query access to the decision-maker, for whom they are learning a policy.
- **Evaluation:** This work evaluates their approach using human simulations (no real human user studies). Mozannar and Sontag (2020) define synthetic experts in the following way: “if the image belongs to the first k classes the expert predicts perfectly, otherwise the expert predicts uniformly over all classes.”

Gao et al. (2021) and Gao et al. (2023):

- **Decision-support set-up:** This work defines two actions: $\mathcal{A} = \{\text{DEFER}, \text{MODEL}\}$. They do not consider the, more practical assumption that the decision-maker will view a model prediction before making a decision themselves. Their formulation is similar to the above but they use offline bandits to learn a suitable policy.

- **Assumptions about decision-maker information:** Gao et al. (2021) assume that understanding decision-maker’s expertise (at a population-level, not at a individual-level) can help learn better routing functions (i.e., defer only when appropriate). Gao et al. (2023) assume access to a decision history for each decision-maker.
- **Evaluation:** They run a human subject experiment to collect offline annotations, which can be used to learn when to defer to decision-makers. Gao et al. (2023) goes further to personalize a deferral policy based on offline annotations for each decision-maker.

Bordt and Von Luxburg (2022):

- **Decision-support set-up:** This work’s set-up can be considered a two-action setting of our formulation, where $\mathcal{A} = \{\text{DEFER}, \text{SHOW}\}$; however, they are concerned with the learnability of such a set up. They do not devise algorithms for this setting, as they are only focused on its theoretical formulation.
- **Assumptions about decision-maker information:** They assume the decision-maker has access to information not contained in the input but still important to the task.
- **Evaluation:** This is a theory paper, containing neither computational nor human subject experiments.

Noti and Chen (2023):

- **Decision-support set-up:** This work’s set-up can be considered as a two-action setting of our formulation, where $\mathcal{A} = \{\text{DEFER}, \text{SHOW}\}$. This is not an online algorithm and as such, the policy does not update.
- **Assumptions about decision-maker information:** They assume access to a dataset of human decisions and that all decision-makers are similar (i.e., they deploy one policy for all decision-makers).
- **Evaluation:** This work is one of few that runs a user study to evaluate their (fixed) policy on unseen decision-makers.

Babbar, Bhatt, and Weller (2022):

- **Decision-support set-up:** This work considers the two-action setting of our formulation, where $\mathcal{A} = \{\text{DEFER}, \text{CONFORMAL}\}$. Their policy is learned offline, is the same for all decision-makers, and is not updated in real-time based on decision-maker behavior.
- **Assumptions about decision-maker information:** They use CIFAR-10H (Peterson et al. 2019) to learn a population-level deferral policy. This assumes that we have annotations for each decision-maker for every datapoint and assumes that all new decision-makers have the same expertise profiles as the population average.
- **Evaluation:** This work runs a user study to evaluate their (fixed) policy. They show the benefits of `DEFER+CONFORMAL` over `CONFORMAL` or `SHOW` alone.

Wolczynski, Saar-Tsechansky, and Wang (2022):

- **Decision-support set-up:** This work considers two actions per our formulation, where $\mathcal{A} = \{\text{DEFER}, \text{SHOW}\}$. They learn a rule-based policy offline for each decision-maker.

- **Assumptions about decision-maker information:** They simulate human behavior by considering explicit functions of how human expertise may vary in input space.
- **Evaluation:** While this work does consider the human to be the final decision-maker, they only validate their proposal in simulation, not on actual human subjects.

Ma et al. (2023):

- **Decision-support set-up:** This work considers two actions per our formulation, where $\mathcal{A} = \{\text{DEFER}, \text{SHOW}\}$. They learn a tree-based and rule-based policy offline for the population but permit one-off editing of these policies.
- **Assumptions about decision-maker information:** They assume access to offline data to initialize their policies, which are then editable. They do not automatically learn online from user behavior over future interactions.
- **Evaluation:** They run extensive human subject experiments to show the benefit of fixed policies, learned from a population and edited by each decision-maker. On models trained on simple tabular UCI datasets, they qualitatively study a decision-maker’s trust and perception of assistance.

Buçinca et al. (2024):

- **Decision-support set-up:** This work considers four actions per our formulation, where $\mathcal{A} = \{\text{DEFER}, \text{EXPLAIN}, \text{CLICK}, \text{SHOW}, \}$. They learn a reinforcement learning policy offline for each decision-maker. This requires having data for each action.
- **Assumptions about decision-maker information:** They require a purely exploratory phase in their learning procedure: this prior data can then be used to learn the policy.
- **Evaluation:** They run human subject experiments on a toy task for assigning exercises to characters, picking between two classes. This differs from our realistic MMLU setting where optionality is higher as well.

We now list various forms of support that can be included in the action space of our problem formulation. The design of the action space is up to domain experts, who can decide not only which actions are feasible but also how much cost to assign to each form of support.

- **DEFER:** This form of support is equivalent to **no support**. Decision-makers are asked to make a decision without any assistance. The machine learning community has studied how to identify when to defer to a subset of examples to humans based on human strengths (Bansal et al. 2021a; Wilder, Horvitz, and Kamar 2021) and/or model failures (Chow 1957; Geifman and El-Yaniv 2017). The premise of such an action would be to allow human decision-makers to be unaided and squarely placing decision liability on the individual.
- **SHOW:** In many settings, machine learning (ML) models are trained to do prediction tasks similar to the decision-making task prescribed to the human, or in the case of foundation models (Bommasani et al. 2021), ML systems can be adapted to aid decision-making, even if the task was not specifically prescribed at train-time (Yang et al. 2023). In essence, a machine learning model prediction, or associated generation (e.g., a code snippet (Mozannar et al.

2022)) would be shown to aid an individual decision-maker. This has been shown to help improve decision-maker performance. The following are variations of showing a model prediction to a decision-maker.

- **CONFORMAL:** For classification tasks, only displaying the most likely label may not lead to good performance due to various reasons, including uncertainty in the modeling procedure (Vovk, Gammerman, and Shafer 2005; Bondi et al. 2022); however, such uncertainty can be communicated to decision-maker by showing a prediction set to experts (Babbar, Bhatt, and Weller 2022). Such a prediction set might be generated using conformal prediction, which guarantees the true label lies in the set with a user-specified error tolerance (Bates et al. 2021; Straitouri et al. 2022).
- **CONFIDENCE:** Instead of translating the uncertainty into a prediction set (or interval), one could simply show the confidence or uncertainty of the prediction, which may manifest as displaying probabilities, standard errors, or entropies (Spiegelhalter 2017; Bhatt et al. 2021). The visualization mechanism used for displaying confidence may alter the decision-maker’s performance (Hullman et al. 2018; Zhang, Liao, and Bellamy 2020).
- **EXPLAIN:** In addition to providing a model prediction, many have considered showing an explanation of model behavior, examples of which include feature attribution (Ribeiro, Singh, and Guestrin 2016; Buçinca et al. 2020), sample importance (Kim, Rudin, and Shah 2014; Jeyakumar et al. 2020), counterfactual explanations (Ustun, Spangher, and Liu 2019; Antoran et al. 2020), and natural language rationales (Ehsan et al. 2018; Camburu et al. 2018). Displaying such explanations to end users has had mixed results on how decision-making performance is affected (Chen et al. 2022; Lai et al. 2022). Worryingly, in many settings, showing some types of explanations may lead to to over-reliance on models by giving the perception of competence (Buçinca et al. 2020; Zerilli, Bhatt, and Weller 2022; Chen et al. 2023).
- **CONSENSUS:** One can also depict forms of support that are independent of any model, for instance, presenting the belief of one or more humans. Belief distributions can be constructed by pooling over many different humans’ “votes” for what a label ought to be, e.g., (Peterson et al. 2019; Beyer et al. 2020; Uma, Almana, and Poesio 2022; Uma et al. 2020; Gordon et al. 2021, 2022), or by eliciting distributions over the likely label directly from each individual human (Collins, Bhatt, and Weller 2022; Collins et al. 2023a). These consensus distributions permit the expression of uncertainty *without any model*. However, the elicitation of this form of support may be costly and humans may be fallible in the information they provide, e.g., due to direct labeling errors (Dawid and Skene 1979; Augustin et al. 2017; Whitehill et al. 2009; Wei et al. 2022), or miscalibrated confidence (O’Hagan et al. 2006; Collins et al. 2023a; Lichtenstein, Fischhoff, and Phillips 1977; Tversky and Kahneman 1996).
- **ADDITIONAL:** While much of this paper focused on support that provides decision-makers with label information,

decision support may also entail acquiring or displaying additional contextual information (e.g., new features (Bakker et al. 2021)) or requesting previously unseen features, for instance, through additional medical diagnostics (Harrell et al. 1982; Mylonakis et al. 2000). This flavor of support can be varied structurally, ranging from the results of a search query (Nakano et al. 2021) to hierarchical information like exposing the subsidiary ownership structure for multinational corporations (Erramilli 1996). In terms of the cost, some pieces of additional information may require additional cost, or certification if pertaining to sensitive attributes.

Prior work on multi-objective contextual bandits. We summarize why some theoretical work on multi-objective contextual bandits cannot be directly applied to our problem formulation. In their study, Tekin and Turğay (2018) addressed a contextual multi-armed bandit problem with two objectives, where one objective dominates the other. Their aim was to maximize the total reward in the non-dominant objective while ensuring that the dominant objective’s total reward is also maximized. However, our specific case requires the minimization of the total expected cost of the support policy while ensuring that the expected accuracy of the decision-maker under the policy remains above a certain threshold. Therefore, the techniques presented by here cannot be directly applied to our scenario. Turgay, Oner, and Tekin (2018) investigated the multi-objective contextual bandit problem with similarity information. Their approach relies on the assumption that a Lipschitz condition holds for the set of feasible context-arm pairs concerning the expected rewards for all objectives and that the learning algorithm has knowledge of the corresponding distance function (see Assumption 1 of their paper).

Additional Details on Problem Formulation

Cost-agnostic Setting.

The optimization problem in the standard setting, where the only objective relates to expected loss, can be written as follows:

$$\begin{aligned} \min_{\pi \in \Pi} L_h(\pi) &= \min_{\pi \in \Pi} \mathbb{E}_{(x,y) \sim \mathcal{P}} [\mathbb{E}_{A_i \sim \pi(x)} [\ell(y, h(x, A_i))]] \\ &\stackrel{(a)}{=} \min_{\pi \in \Pi} \mathbb{E}_{(x,y) \sim \mathcal{P}} \left[\sum_{i=1}^k \pi(x)_{A_i} \cdot \ell(y, h(x, A_i)) \right] \\ &\stackrel{(b)}{=} \min_{\pi \in \Pi} \mathbb{E}_x \left[\sum_{i=1}^k \pi(x)_{A_i} \cdot \mathbb{E}_{y|x} [\ell(y, h(x, A_i))] \right] \\ &\stackrel{(c)}{=} \min_{\pi \in \Pi} \mathbb{E}_x \left[\sum_{i=1}^k \pi(x)_{A_i} \cdot r_{A_i}(x; h) \right], \end{aligned}$$

where (a) is due to the notation $\pi(x)_{A_i} := \mathbb{P}[A_i \sim \pi(x)]$, (b) is due to the properties of expectation, and (c) is due to the notation $r_{A_i}(x; h) := \mathbb{E}_{y|x} [\ell(y, h(x, A_i))]$. Then, by noting the fact that the expression $\mathbb{E}_x \left[\sum_{i=1}^k \pi(x)_{A_i} \cdot r_{A_i}(x; h) \right]$

can be optimized independently for each $x \in \mathcal{X}$, we can rewrite the above optimization problem as follows, for each $x \in \mathcal{X}$:

$$\min_{\pi(x) \in \Delta(\mathcal{A})} \sum_{i=1}^k \pi(x)_{A_i} \cdot r_{A_i}(x; h) = \min_{A_i \in \mathcal{A}} r_{A_i}(x; h).$$

Thus, an optimal policy for the above optimization problem is: $\pi^*(x) \in \arg \min_{A_i \in \mathcal{A}} r_{A_i}(x; h)$ with random tie-breaking.

Implementations of Modiste

The human decision-making process with various forms of support can be effectively modeled as a stochastic contextual bandit problem. In this model, the diverse forms of support represent the available arms, and \mathcal{X} represents the context space. For our investigation, we leverage two simple and efficient techniques from the existing contextual bandit literature: LinUCB (Li et al. 2010) and KNN-UCB (Guan and Jiang 2018). It’s worth noting that while any contextual bandit algorithm could be employed, we chose these two simpler methods as they have demonstrated their effectiveness in empirically showcasing the utility of our online decision support policy learning framework.

We present specific implementations of the Modiste algorithm (see Algorithm 1) using LinUCB and KNN-UCB in Algorithms 2 and 3, respectively. Importantly, these algorithms naturally inherit the regret bounds associated with LinUCB and KNN-UCB, as discussed below.

λ Selection Strategies

There are many ways to select the λ to use on unseen decision-makers using a population of decision-makers. We outline three such strategies below. Note we use B in the main paper.

- A. **Most likely λ .** For each simulator, we identify the set of $\{\lambda_{\text{sim-}j}\}$, which yield policies that meet $L_{h_{\text{sim-}j}}^{\text{opt}} + \epsilon$. We then take the λ that occurs the *most often* across simulators. If no policy meets the threshold for $h_{\text{sim-}j}$, we select the policy closest to $L_{h_{\text{sim-}j}}^{\text{opt}}$, which can be computed given r_{A_i} for all x for each simulated decision-maker.
- B. **Most likely λ with lowest cost.** For each simulator, we identify the set of $\{\lambda_{\text{sim-}j}\}$, which yield policies that meet $L_{h_{\text{sim-}j}}^{\text{opt}} + \epsilon$, and select the λ whose policy has the least expected cost. Then, we identify the most common value across simulators. While the set of values here is a subset of the selection strategy A, a cost-aware selection strategy may identify a parameter that leads to a lower cost for new decision-makers.
- C. **Conservative λ .** For each simulator, we identify $\lambda_{\text{sim-}j}$ which is the minimum parameter that meets $L_{h_{\text{sim-}j}}^{\text{opt}} + \epsilon$. We then take $\max_j \lambda_{\text{sim-}j}$ over all simulated decision-makers. In the absence of suitable population-level information, this strategy is similar to picking a conservative value of λ that prioritizes performance.

Algorithm 2: Modiste using LinUCB

- 1: **Input:** trade-off parameter λ ; human decision-maker h ; cost function $c : \mathcal{A} \rightarrow [0, 1]$; UCB parameter α
 - 2: **Initialization:** data buffer $\mathcal{D}_0 = \{\}$; $\mathbf{A}_a = \mathbf{I}_{p \times p}$ and $\mathbf{b}_a = \mathbf{0}_{p \times 1}$ for all $a \in \mathcal{A}$; $\{\theta_a = (\mathbf{A}_a)^{-1} \mathbf{b}_a : a \in \mathcal{A}\}$; human prediction error values $\{\hat{r}_{a,0}(x; h) = \langle \theta_a, x \rangle : x \in \mathcal{X}, a \in \mathcal{A}\}$; initial policy $\pi_1(x)_a = 1/|\mathcal{A}|$ for all $a \in \mathcal{A}$
 - 3: **for** $t = 1, 2, \dots, T$ **do**
 - 4: data point $(x_t, y_t) \in \mathcal{X} \times \mathcal{Y}$ is drawn iid from \mathcal{P} (normalized s.t. $\|x_t\|_2 \leq 1$)
 - 5: support $a_t \in \mathcal{A}$ is selected using policy π_t
 - 6: human makes the prediction \tilde{y}_t based on x_t and a_t
 - 7: human incurs the loss $\ell(y_t, \tilde{y}_t)$
 - 8: update the buffer $\mathcal{D}_t \leftarrow \mathcal{D}_{t-1} \cup \{(x_t, a_t, \ell(y_t, \tilde{y}_t))\}$
 - 9: update the decision support policy:

$$\begin{aligned} \mathbf{A}_{a_t} &\leftarrow \mathbf{A}_{a_t} + x_t x_t^\top \\ \mathbf{b}_{a_t} &\leftarrow \mathbf{b}_{a_t} + r_t x_t \\ \theta_a &\leftarrow (\mathbf{A}_a)^{-1} \mathbf{b}_a \text{ for all } a \in \mathcal{A} \\ \hat{r}_{a,t}(x; h) &\leftarrow \langle \theta_a, x \rangle \text{ for all } a \in \mathcal{A} \end{aligned} \tag{Step 1}$$
 - $$\pi_{t+1}(x) \leftarrow \arg \min_{a \in \mathcal{A}} \lambda \cdot \hat{r}_{a,t}(x; h) + (1 - \lambda) \cdot c(a) - \alpha \cdot \sqrt{x^\top (\mathbf{A}_a)^{-1} x} \tag{Step 2}$$
 - 10: **end for**
 - 11: **Output:** policy $\pi_\lambda^{\text{alg}} \leftarrow \pi_{T+1}$
-

Additional Experimental Details

Datasets

Computational Only. Two tasks (Synthetic-2A and CIFAR-2A) are used only in the computational experiments, so we describe them abstractly. Both have the same set-up, but have different underlying data generating distributions. Consider learning a decision support policy in a setting where there are *two* forms of support available: $\mathcal{A} = \{A_1, A_2\}$, hence CIFAR-2A. Let $c(A_1) = 0$ and $c(A_2) = 0.5$. We simulate a decision-maker’s behavior under each r_{A_i} across 3 classes for Synthetic/CIFAR. We instantiate the m decision-makers in the population data using human simulations, where we randomly sample $r_{A_i}(x; h)$ from a distribution for each h in the population.

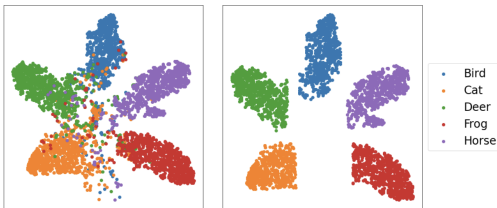


Figure 7: We depict the latent space of the CIFAR subset used. Embeddings without filtering (left) and after filtering out points that violate separability of classes (right). We use the embeddings on the right for our Synthetic-2A task and the left for the natural CIFAR tasks.

CIFAR. To explore the performance of our algorithms in both separable and non-separable settings, we construct two subvariants of the CIFAR-10 (Krizhevsky 2009) image dataset. As depicted in Figure 7, we subsample from

the CIFAR embeddings to create linearly separable classes. Embeddings are constructed by running t-SNE on the 512-dimensional latent codes extracted by the penultimate layer of a variant of the VGG architecture (VGG-11) (He et al. 2016) trained on the animal class subset of CIFAR; the model attained an accuracy of 89.5%. We filter the original 10 CIFAR classes to only include those involving animals (Birds, Cats, Deers, Dogs, Frogs, and Horses). We consider at most 5 such classes in our experiments (dropping Dog).

MMLU We consider questions from four topics of MMLU (elementary mathematics, high school biology, high school computer science, and US foreign policy). Topic names match those proposed in (Hendrycks et al. 2020). We select topics to cover span an array of disciplines across the sciences and humanities, as discussed in Appendix . We use questions in the MMLU test set for each topic that are at most 150 characters long. We limit the length of questions to facilitate readability in our human user studies and wanted to maximize parity between our computational and human experiments by considering the same set of questions across both set-ups. This yields 264, 197, 98, and 47 questions for the elementary mathematics, high school biology, US foreign policy, and high school computer science topics, respectively. We emphasize that in CIFAR, our forms of support operate in label space – in contrast, with MMLU, support selection is in *covariate* (topic) space – further highlighting the flexibility of our adaptive support paradigm.

We leverage OpenAI’s LLM-based embedding model (text-embedding-ada-003), to produce embeddings over the question prompts. Embedding vectors extracted via OpenAI’s API are by default length 1536; we apply t-SNE, like in the CIFAR tasks, to compress the embeddings into two-dimensional latent codes per example. Nicely, these latents are already separable (see Figure 5; no post-filtering is

Algorithm 3: Modiste using online KNN

- 1: **Input:** trade-off parameter λ ; human decision-maker h ; cost function $c : \mathcal{A} \rightarrow [0, 1]$; warm-up steps W ; number of neighbours K ; exploration parameter γ
 - 2: **Initialization:** data buffer $\mathcal{D}_0 = \{\}$; human prediction error values $\{\hat{r}_{a,0}(x; h) = 0.5 : x \in \mathcal{X}, a \in \mathcal{A}\}$; initial policy $\pi_1(x)_a = 1/|\mathcal{A}|$ for all $a \in \mathcal{A}$
 - 3: **for** $t = 1, 2, \dots, T$ **do**
 - 4: data point $(x_t, y_t) \in \mathcal{X} \times \mathcal{Y}$ is drawn iid from \mathcal{P}
 - 5: support $a_t \in \mathcal{A}$ is selected using policy π_t
 - 6: human makes the prediction \tilde{y}_t based on x_t and a_t
 - 7: human incurs the loss $\ell(y_t, \tilde{y}_t)$
 - 8: update the buffer $\mathcal{D}_t \leftarrow \mathcal{D}_{t-1} \cup \{(x_t, a_t, \ell(y_t, \tilde{y}_t))\}$
 - 9: update the decision support policy:

$$\begin{aligned} \mathcal{N}(x) &\leftarrow \text{K neighbouring data points for } x \text{ in } \mathcal{D}_t \\ \mathcal{N}_a(x) &\leftarrow \{(x_i, a_i, \ell(y_i, \tilde{y}_i)) : (x_i, a_i, \ell(y_i, \tilde{y}_i)) \in \mathcal{N}(x) \text{ and } a_i = a\} \quad \text{for all } a \in \mathcal{A} \\ \hat{r}_{a,t}(x; h) &\leftarrow \frac{1}{|\mathcal{N}_a(x)|} \cdot \sum_{(x_i, a_i, \ell(y_i, \tilde{y}_i)) \in \mathcal{N}_a(x)} \ell(y_i, \tilde{y}_i) \quad \text{for all } a \in \mathcal{A} \text{ with } |\mathcal{N}_a(x)| > 0 \end{aligned} \quad \text{(Step 1)}$$
 - 10: $\pi_{\text{rand}}(x)_a \leftarrow \frac{1}{|\mathcal{A}|}$ for all $a \in \mathcal{A}$
 - 11: $\pi_{\text{knn}}(x) \leftarrow \arg \min_{a \in \mathcal{A}} \lambda \cdot \hat{r}_{a,t}(x; h) + (1 - \lambda) \cdot c(a)$
 - 12: $\pi_{t+1}(x) \leftarrow \pi_{\text{rand}}(x)$ if $t \leq W$ (Step 2)
 - 13: $\pi_{t+1}(x) \leftarrow \gamma \cdot \pi_{\text{rand}}(x) + (1 - \gamma) \cdot \pi_{\text{knn}}(x)$ if $t > W$ (Step 2)
 - 14: **end for**
 - 15: **Output:** policy $\pi_\lambda^{\text{alg}} \leftarrow \pi_{T+1}$
-

applied to ensure separability).

CIFAR Task Set-up

We consider a 5-class subset of CIFAR (Bird, Cat, Deer, Frog, and Horse), as discussed in Appendix 5. We instantiate two forms of support: 1) a simulated AI model which provides a prediction for the image class, and 2) a consensus response derived from real humans, derived from the approximately 50 human annotators from CIFAR-10H (Peterson et al. 2019; Battleday, Peterson, and Griffiths 2020), presented as a distribution over the 5 classes.

We treat the original CIFAR-10 test set labels as the “true” labels and only include images for which the original CIFAR-10 label matches the label deemed most likely from the CIFAR-10H annotators (discrepancy was a rare occurrence, only 1.1% of the 5000 images considered). We sample a pool of 300 such images, and construct three different batches of 100 images. Participants are assigned to one batch of 100 images. Images per batch are sampled in a class-balanced fashion (i.e., 20 images for each of the 5 categories). Images are shuffled for each participant. The same latent codes (z_t) used in the computational experiments are employed for the user studies. For CIFAR, we

⁵We explored a 3 class variant for HSEs to directly match the computational experiments; however, we realized that participants were able to figure out that which classes were impoverished, raising the base rate of correctly categorizing such images. Such behavior again highlights the need to carefully consider real human behavior in adaptive decision support systems.

define the support costs as: $c(\text{HUMAN ALONE}) = 0$ and $c(\text{MODEL}) = c(\text{CONSENSUS}) = 0.5$.

Corruptions and Support Design We want to study whether our algorithms can properly learn which forms of decision support are actually needed by real humans. We therefore need to ensure that the task is sufficiently rich such that humans do *need* support (and the existing forms of support which can be of value). To mimic such a setting in CIFAR, we deliberately corrupt images of all classes except one (i.e., Birds⁶) when presenting images to the user. Corruptions are formed via a composition of natural adversarial transformations proposed in Hendrycks et al. (2020), specifically shot noise ontop of glass blur. This enables us to check that our algorithms are able to properly recommend support for all other classes, as a human will be unable to decide on image category unassisted. Example corrupted images can be seen in Figure 3.

To ensure that the available forms of support have different regions of strength, we enforce that each form of support is only good at two of the five classes. In the case of the simulated AI model, we return the “true” class whenever the image is a Deer or Cat classes, and return one of the incorrect classes for all other images. For the consensus labels, we use the CIFAR-10H distribution derived from 50 annotators when

⁶We further disambiguate the non-corrupted bird class by upsampling to 160x160 images via Lanczos-upsampling following (Peterson et al. 2019; Battleday, Peterson, and Griffiths 2020; Collins, Bhatt, and Weller 2022) before presenting them to participants.

the image is a Horse or Frog. As the CIFAR-10H labels were originally collected over all 10 CIFAR classes, sometimes an annotation was endorsed for a class outside of the 5 we consider; in that case, we discard the annotations assigned to those classes and renormalize the remaining distribution (on average, $< 2\%$ of the original labeling mass was discarded per image). For all other classes, we intend the consensus to be an unhelpful form of support, as such, for images in the Bird, Deer, and Horse class, we return a uniform distribution (i.e., providing no information to the participant).

MMLU Task Set-up

Participants respond to 60 multiple choice questions, which were balanced by topic (15 questions per topic). Participants are assigned to one of three possible batches of 60 such questions. Order is shuffled. Participants are informed of the topic associated with each question (e.g., that the question was about biology). We implement a 10 second delay between when the question is presented and when the participant is allowed to submit their response to encourage participants to try each problem in earnest. For MMLU, we let the support costs be $c(\text{HUMAN ALONE}) = 0$ and $c(\text{MODEL}) = 0.1$.

Topic Selection We ran several pilot studies with `Modiste` to determine people’s base performance on a subset of MMLU topics. We intended to select a diverse set of topics such that it was unlikely any one participant would excel at all topics – as many of the topics were specialized and challenging (Hendrycks et al. 2020) – but also varied enough that participants may be strong in at least one area. We found that a large number of participants achieved reasonable performance on elementary mathematics, and that a sufficient number of participants also excelled at questions in the high school biology, US foreign policy, and high school computer science topics – though usually not all together.

We also factored in `InstructGPT-3.5`’s performance while deciding on the topics. To check whether our adaptive decision support algorithms are effective at learning good policies – like with CIFAR – it is helpful to have support available that is effective, should someone be unable to answer adequately alone. As a result, we looked more sympathetically on categories where model accuracy was already high.

However, the real-world is not so perfect: there may not be high-performing support available when a human struggles to make a decision. As such, we also deliberately forced down the accuracy of the LLM form of support in the mathematics topic. While we expect that most participants would be able to solve elementary mathematics problems without the aid of the LLM support, should they be unable to, the LLM was not able to help them. We leave further impoverishing studies which mimic real-world support settings for future work.

Question Selection and Model Accuracy The resulting accuracy of the LLM form of support on the questions shown to humans per topic is 29% for elementary mathematics, 89% for high school biology, 87% for US foreign policy, and 91% for high school computer science. We upweighted selection of foreign policy questions that participants in our pilot had gotten correct when constructing the question subset, as we

wanted to ensure that, should a participant have foreign policy experience, they would be able to answer them.

Compute Resources

All computational experiments were run using CPUs (either on local machines or Google Colab), with the exception of training the VGG used for CIFAR embeddings. Here, we accessed a group compute cluster and trained the model for roughly five hours on a Nvidia A100-SXM-80GB GPU.

Additional Computational Experiments

Implications of selecting the trade-off parameter λ (with varying cost structure). We follow the strategies to identify λ for our cost-aware experiments. In Figure 9, we visualized the expected excess loss and cost for each value of λ that is used for our human-informed synthetic decision-makers. Further, as shown in Figure 8, we highlight how only a subset of λ values falls within $\epsilon = 0.05$ of the L_h^{opt} of that individual (e.g., in Figure 8). We also find that `Modiste-KNN` has more monotonic and controllable behavior as λ increases, while λ seems to have less of an effect on `Modiste-LinUCB`. We note that the set of λ values that fall within the red region is affected by the choice of cost structure, as shown in Figure 8. Thus, any changes to the cost structure would imply the need to redo the hyper-parameter tuning process.

Additional Experiments on Datasets. In Table 4, we provide additional computational results for CIFAR-2A and MMLU-2A in the cost-aware setting. We find that `Modiste` successfully personalizes decision support policies that trade-off cost and performance effectively. We note that in all of our experiments, we fix the exploration parameters in `LinUCB` and `KNN` (i.e., $\alpha = 1$ and $\gamma = 0.1$ respectively). However, we do explore varying these exploration parameters in Table 6.

Varying KNN Parameters. While `LinUCB` does not require identifying additional parameters, `KNN` has two: K which is the number of nearest neighbors to select when estimating the risk of a form of support and W which is the length of the warm-up period. In Table 7, we show that as long as K is reasonably sized (i.e. $K > 3$), the performance of `KNN` does not vary too much across datasets.

Varying Embedding Size. In the main text, we run computational experiments using a two-dimension t-SNE embedding. In Table 8 for CIFAR-2A, we consider how `Modiste` would behave when we vary dimensionality of \mathcal{X} . We extract higher dimensional embeddings from animal-class trained VGGs (see above) with varied penultimate layer widths, where width matches embedding size. While we opt for t-SNE embeddings, in the main paper, to provide a clearer visualizations, we find that strong performance holds even for high-dimensional embeddings. We expect that even larger embedding dimensions will permit `Modiste` to work in a variety of real-world contexts, but may come at the added cost of an increase in the number of required interactions, if we learn with no prior assumptions on the decision-maker’s expertise profile.

$|\mathcal{A}| > 3$ **Experiments.** We now demonstrate how `Modiste` behaves when we increase the number of forms of support available to a decision-maker. Using the same set-up and algorithm-specific hyperparameters as Table 1, we convert the CIFAR setting to five forms of support (one for each class), resulting in CIFAR-5A, and convert the MMLU setting to four forms of support (one for each topic) resulting in MMLU-4A. In Table 9, we report $L_h(\pi)$ at three time steps: $t = 50, 100, 250$. For CIFAR, we find that KNN significantly outperforms given more interactions, which is expected when we increase $|\mathcal{A}|$. We believe that LinUCB struggles as the t-SNE embedding space is likely not rich enough to capture the intricacies of all five forms of support. Given a larger embedding space, we expect that LinUCB would excel when the number of forms of support is increased. For MMLU, both LinUCB and KNN perform well by the 250th interaction: KNN is very good at lowering $L_h(\pi)$ on this task. In all, this experiment assures us that careful design of decision support can permit us to use `Modiste` when we have a larger set of potential forms of support.

While we include experiments with larger $|\mathcal{A}|$ here, we note that higher set sizes may also be problematic for two reasons: 1) decision-makers may struggle under many forms of support (Kalis, Kaiser, and Mojzisch 2013), and 2) as size increases, we find that the number of interactions required to learn an accurate personalized policy also increases.

Sensitivity to choice of T . In Figure 10, we consider a setting of learning a policy with three forms of support: $\mathcal{A} = \{A_1, A_2, A_3\}$. Let $c(A_1) < c(A_2) = c(A_3)$. This is an analogous setup to what we do in our human subject experiments in Section . We indicate the simulated human expertise profiles in the caption. We show how performance on a random sample of 100 points from a held-out set varies with time while learning a decision support policy. In general, we find that the more forms of support to learn, the longer it may take for the online algorithms to “converge.” For various simulations, KNN is more consistent in learning a decision support policy efficiently.

Additional User Study Details and Results

CIFAR Algorithm Parameters For KNN, we take $K = 8$, $W = 25$, and $\epsilon = 0.1$; for both algorithms, we let $\alpha = 1$. Cost of either model arm is 0.5. For each algorithm, we consider two different settings of λ ($\lambda \in \{0.75, 1.0\}$ and $\in \{0.85, 1.0\}$ for KNN and LinUCB respective), selected using the hyper-parameter selection methods described in the main text.⁷

MMLU Algorithm Parameters We use the same parameters as in the CIFAR task, with the exception that we set the cost of support (i.e., the LLM arm) to 0.1. Additionally, we employ different λ – $\lambda \in \{0.75, 1.0\}$ for KNN and $\lambda \in \{0.95, 1.0\}$ for LinUCB – selected using the hyper-parameter selection methods described in the main text.

⁷Due to a server-side glitch, 6 of the 125 recruited participants received incorrect feedback on $\leq 2\%$ of trials.

Further Results

Visualizing Learned Policies. We provide additional details on how the policy generalization snapshots in Figures 4 and 5 are constructed. We save out the parameters learned by each algorithm while a participant interacts with `Modiste`. After the 60 or 100 trials (depending on which task they participated in), we load in the final state of parameters. We sample the embeddings of *unseen points* from the respective task dataset (as described in Appendix) and pass these through the respective algorithm (LinUCB or KNN, depending on which variant the participant was assigned to) – yielding a recommended form of support for said embedding. We color the latent by the form of support. We draw randomly 250 such unseen examples for CIFAR, and 100 for MMLU, when computing the policy recommendations.

We include snapshots for participants, across both tasks, in the main text. We depict all CIFAR examples and a random sampling of 7 of the 10 participants per variant for MMLU.

Cumulative results. We also report in Table 10 the expected loss and cost across all trials. In general, we find similar trends as Table 3.

Participant Comments Hint at Mental Models of AI In a post-experiment survey where we permitted participants to leave general comments, we observed that several participants in our MMLU task noted that their responses were biased by the AI. We include a sampling of comments provided by participants which we found particularly revealing. We believe that these responses motivate the need for further study of how users’ mental models of AI systems inform their decision-making performance, particularly in light of the rapidly advancing and public-facing foundation models (Bommasani et al. 2021).

- ‘‘I thought the AI answers went against my previous notions about what an AI would be proficient at answering. I thought an AI would excel at anything where there is a set answer such as math, computer science coding question, and biology textbook definitions. Then I expected it to absolutely fail at political, and historical questions. Since they can be more opinionated and not have a definitive answer. However, the AI struggled with math and excelled in the other topics. So I was actively not choosing to agree with the AI on any math where I could also easily check its work and was heavily relying on it for everything else [...] I knew nothing about any question on computer science, so I mainly relied on AI for answers on that topic.’’
- ‘‘AI seemed to me more helpful in topics I didn’t know, but sometime I trusted it too much, instead of thinking the answer through’’

- ``The AI had me second guessing myself sometimes so it affected my answers occasionally.''
- ``Anything highlighted with the AI I was confident that would be the right answer.''

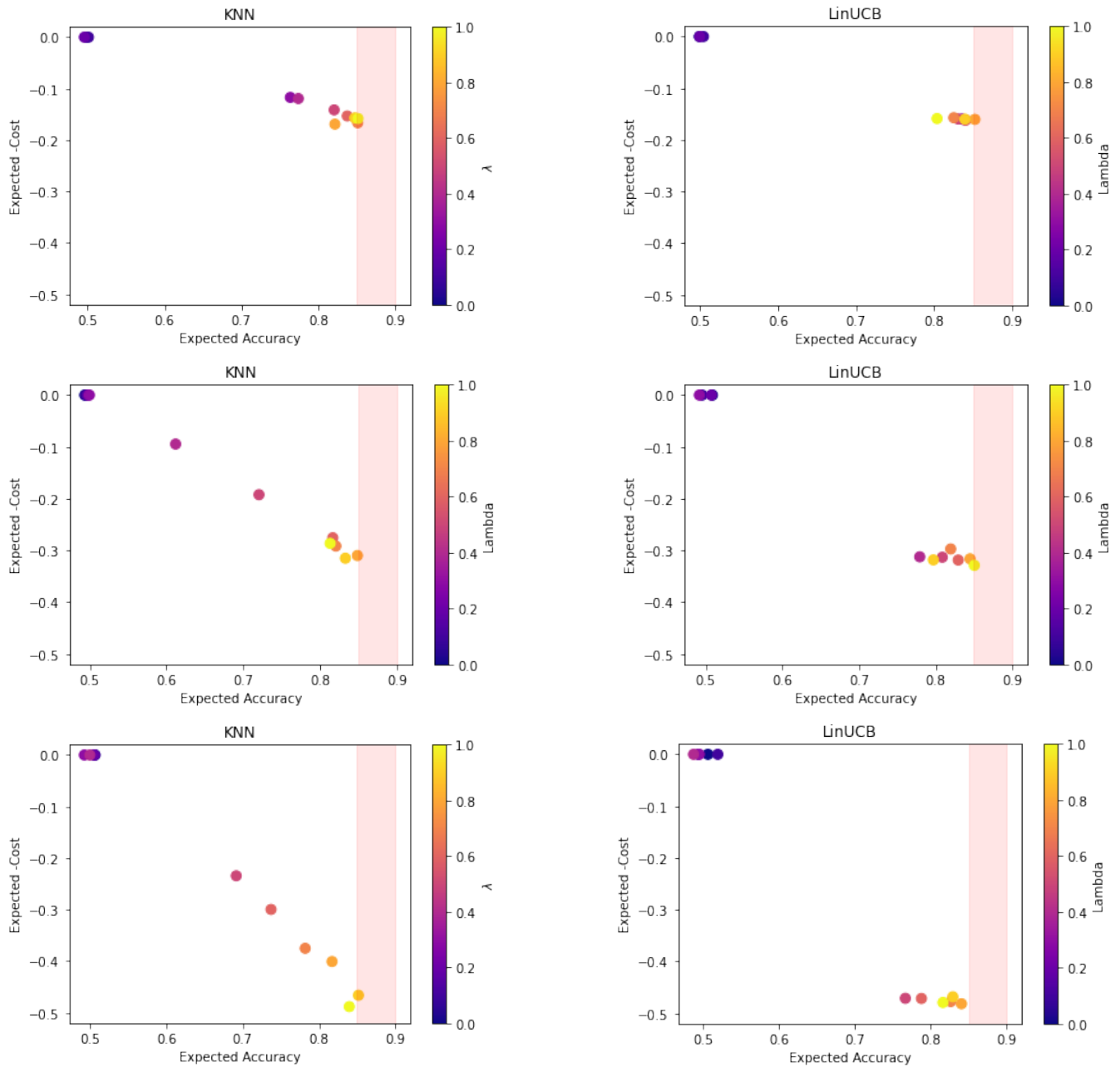


Figure 8: We plot the expected accuracy and the negative of the expected cost for an individual sampled from the Synthetic-2A dataset for $\lambda \in [0, 1]$. The ideal policy would lie in the far right corner. The red region denotes policies that fall within ϵ of the best risk for the sampled individual. We observe that there exists a policy that lies in the red region for both `Modiste-KNN` and `Modiste-LinUCB`. We also vary the cost structure (i.e., the cost of $A_1 = 0$ and the cost of $A_2 = 0.25, 0.5, 0.75$ in the first, second, and third row respectively).

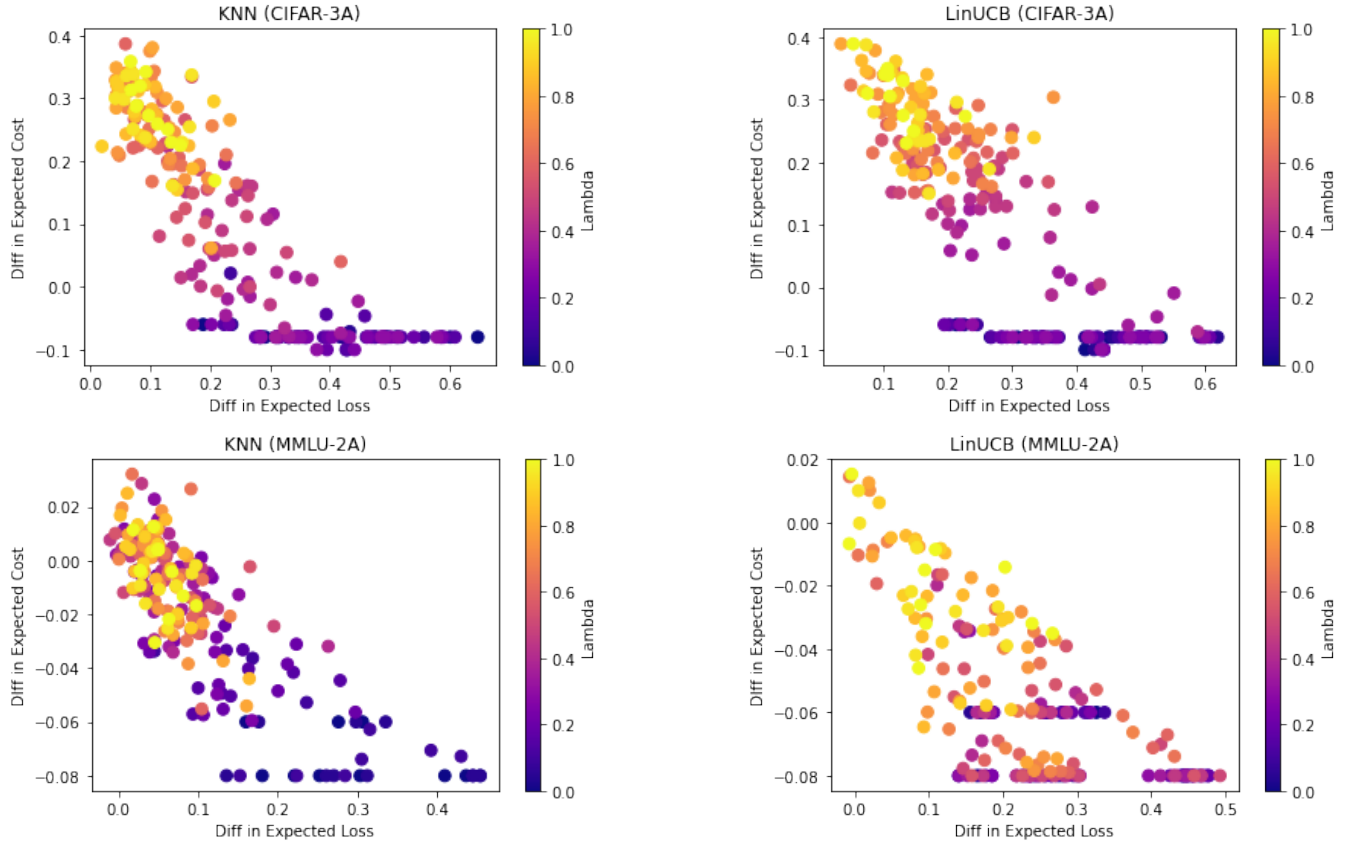
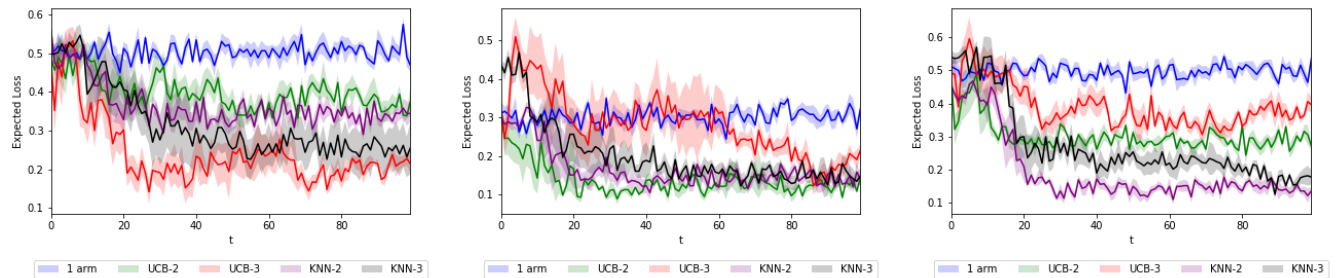


Figure 9: Top is CIFAR-3A and Bottom is MMLU-2A. For each of the $N = 10$ simulators, we instantiate using the population data, we compute the difference in expected loss between the optimal policy for that simulator and the learned policy for all values of $\lambda \in [0, 1]$ in increments of 0.05, and compute the difference in expected cost in the same manner. For KNN, we observe overlap between many values of λ that all come within ϵ of the Best Risk: this implies we can use lower values of λ to potentially achieve the desired level of performance. For LinUCB, we find that large values of λ are required to achieve a suitable level of performance.



$$r_{A_1} = [0.1, 0.7, 0.7]$$

$$r_{A_2} = [0.7, 0.1, 0.7]$$

$$r_{A_3} = [0.7, 0.7, 0.1]$$

$$r_{A_1} = [0.1, 0.7, 0.1]$$

$$r_{A_2} = [0.7, 0.1, 0.1]$$

$$r_{A_3} = [0.7, 0.7, 0.7]$$

$$r_{A_1} = [0.1, 0.7, 0.7]$$

$$r_{A_2} = [0.7, 0.1, 0.1]$$

$$r_{A_3} = [0.7, 0.7, 0.7]$$

Figure 10: Loss plots over time for human simulations (denoted by r_{A_i}) in the CIFAR-3A setting.

Table 4: Unlike Table 2 where risks come from pilot studies, we instantiate simulated **synthetic** humans, each specified by the human’s loss on each form of support H-ONLY (Human only) and H-MODEL (Human+Model), for MMLU-2A. We report the expected loss $r_h(\pi)$ and the expected cost $c(\pi)$ —for both metrics, lower is better—averaged across the last 10 steps of 100 total time steps along with their standard deviations (across 5 runs). We bold the algorithm that achieves the lowest cost within ϵ of the Best Risk for each human simulation and find that our algorithm outperforms baselines on various simulated humans. For each form of support, we specify risk r over each of the 4 topics for MMLU-2A. We fix the cost structure: $c(\text{H-ONLY}) = 0.0$ and $c(\text{H-MODEL}) = 0.1$. The selected λ values used for Modiste are in Table 5. For Modiste, we select the best policy over a sweep of λ values that minimizes our objective under $\epsilon = 0.05$. We also indicate the values of λ chosen beneath the results table.

Algorithm		$r_{A_1} = [0.7, 0.1, 0.7]$ $r_{A_2} = [0.1, 0.1, 0.1]$		$r_{A_1} = [0.7, 0.1, 0.7]$ $r_{A_2} = [0.1, 0.7, 0.1]$		$r_{A_1} = [0.7, 0.1, 0.7]$ $r_{A_2} = [0.7, 0.7, 0.1]$	
		$L_h(\pi)$	$c(\pi)$	$L_h(\pi)$	$c(\pi)$	$L_h(\pi)$	$c(\pi)$
Synthetic-2A	A ₁ Only	0.51 ± 0.05	0.0	0.50 ± 0.06	0.0	0.50 ± 0.06	0.0
	A ₂ Only	0.10 ± 0.03	0.5	0.30 ± 0.05	0.5	0.50 ± 0.04	0.5
	Population	0.37 ± 0.04	0.13 ± 0.03	0.34 ± 0.05	0.13 ± 0.02	0.49 ± 0.06	0.12 ± 0.03
	Modiste-LinUCB	0.15 ± 0.05	0.31 ± 0.03	0.12 ± 0.04	0.32 ± 0.03	0.34 ± 0.11	0.28 ± 0.07
	Modiste-KNN	0.11 ± 0.04	0.36 ± 0.03	0.13 ± 0.04	0.30 ± 0.03	0.33 ± 0.06	0.21 ± 0.03
	Best Risk	0.1	0.33	0.1	0.33	0.3	0.17
Algorithm		$r_{A_1} = [0.7, 0.1, 0.7]$ $r_{A_2} = [0.1, 0.1, 0.1]$		$r_{A_1} = [0.7, 0.1, 0.7]$ $r_{A_2} = [0.1, 0.7, 0.1]$		$r_{A_1} = [0.7, 0.1, 0.7]$ $r_{A_2} = [0.7, 0.7, 0.1]$	
		$L_h(\pi)$	$c(\pi)$	$L_h(\pi)$	$c(\pi)$	$L_h(\pi)$	$c(\pi)$
CIFAR-2A	A ₁ Only	0.50 ± 0.05	0.0	0.50 ± 0.05	0.0	0.47 ± 0.05	0.0
	A ₂ Only	0.1 ± 0.03	0.5	0.31 ± 0.04	0.5	0.49 ± 0.05	0.5
	Population	0.46 ± 0.07	0.03 ± 0.04	0.43 ± 0.06	0.07 ± 0.03	0.50 ± 0.06	0.03 ± 0.02
	Modiste-LinUCB	0.15 ± 0.04	0.31 ± 0.02	0.14 ± 0.05	0.32 ± 0.02	0.34 ± 0.07	0.25 ± 0.07
	Modiste-KNN	0.14 ± 0.04	0.33 ± 0.06	0.14 ± 0.04	0.32 ± 0.03	0.33 ± 0.05	0.18 ± 0.03
	Best Risk	0.1	0.33	0.1	0.33	0.3	0.17
Algorithm		$r_{A_1} = [0.8, 0.8, 0.1, 0.1]$ $r_{A_2} = [0.2, 0.1, 0.1, 0.2]$		$r_{A_1} = [0.2, 0.8, 0.1, 0.1]$ $r_{A_2} = [0.8, 0.1, 0.1, 0.2]$		$r_{A_1} = [0.2, 0.5, 0.5, 0.8]$ $r_{A_2} = [0.8, 0.1, 0.1, 0.8]$	
		$r_h(\pi)$	$c(\pi)$	$r_h(\pi)$	$c(\pi)$	$r_h(\pi)$	$c(\pi)$
MMLU-2A	H-ONLY ($\pi_{\lambda=0}^*$)	0.45 ± 0.04	0.0	0.33 ± 0.06	0.0	0.51 ± 0.04	0.0
	H-MODEL	0.14 ± 0.02	0.1	0.30 ± 0.05	0.1	0.45 ± 0.04	0.1
	Human Pop	0.45 ± 0.07	0.05 ± 0.01	0.22 ± 0.08	0.06 ± 0.01	0.41 ± 0.04	0.05 ± 0.01
	Modiste-LinUCB	0.15 ± 0.04	0.05 ± 0.06	0.19 ± 0.07	0.05 ± 0.02	0.39 ± 0.08	0.06 ± 0.01
	Modiste-KNN	0.14 ± 0.06	0.04 ± 0.01	0.13 ± 0.04	0.03 ± 0.04	0.33 ± 0.05	0.05 ± 0.01
	Best Risk ($\pi_{\lambda=1}^*$)	0.13	0.05	0.13	0.03	0.3	0.05

Selected λ Values

Algorithm		$r_{A_1} = [0.7, 0.1, 0.7]$ $r_{A_2} = [0.1, 0.1, 0.1]$	$r_{A_1} = [0.7, 0.1, 0.7]$ $r_{A_2} = [0.1, 0.7, 0.1]$	$r_{A_1} = [0.7, 0.1, 0.7]$ $r_{A_2} = [0.7, 0.7, 0.1]$
Synthetic-2A	Modiste-LinUCB	0.4	0.6	0.6
	Modiste-KNN	0.9	0.6	0.6
CIFAR-2A	Modiste-LinUCB	0.4	0.9	0.5
	Modiste-KNN	0.7	0.9	0.6

Algorithm		$r_{A_1} = [0.8, 0.8, 0.1, 0.1]$ $r_{A_2} = [0.2, 0.1, 0.1, 0.2]$	$r_{A_1} = [0.2, 0.8, 0.1, 0.1]$ $r_{A_2} = [0.8, 0.1, 0.1, 0.2]$	$r_{A_1} = [0.2, 0.5, 0.5, 0.8]$ $r_{A_2} = [0.8, 0.1, 0.1, 0.8]$
MMLU-2A	Modiste-LinUCB	1.0	0.9	1.0
	Modiste-KNN	0.3	0.2	0.3

Table 5: The best value of λ that is selected from doing a sweep over $\lambda \in [0, 1]$ that corresponds to the human simulators in Table 2. The column ordering is the same as the main paper.

Algorithm		Best Alone	Second Best Alone	Highest Best Risk	Lowest Best Risk
MMLU-2A	Modiste-LinUCB	0.7	0.65	1.0	0.95
	Modiste-KNN	0.25	0.55	0.35	0.6

Table 6: Vary exploration parameters (α for LinUCB and γ for KNN). We find that LinUCB generally performs better when exploration increases and KNN generally performs better when exploration decreases.

Algorithm		$r_{A_1} = [0.7, 0.1, 0.7]$ $r_{A_2} = [0.1, 0.1, 0.1]$		$r_{A_1} = [0.7, 0.1, 0.7]$ $r_{A_2} = [0.1, 0.7, 0.1]$		$r_{A_1} = [0.7, 0.1, 0.7]$ $r_{A_2} = [0.7, 0.7, 0.1]$	
		$r_h(\pi)$	$c(\pi)$	$r_h(\pi)$	$c(\pi)$	$r_h(\pi)$	$c(\pi)$
Synthetic-2A	Modiste-LinUCB ($\alpha = 0.1$)	0.14 \pm 0.04	0.33 \pm 0.02	0.19 \pm 0.09	0.32 \pm 0.02	0.34 \pm 0.10	0.21 \pm 0.07
	Modiste-LinUCB ($\alpha = 10$)	0.13 \pm 0.04	0.32 \pm 0.03	0.12 \pm 0.03	0.33 \pm 0.02	0.30 \pm 0.05	0.23 \pm 0.07
	Modiste-KNN ($\gamma = 0.01$)	0.12 \pm 0.04	0.35 \pm 0.06	0.19 \pm 0.08	0.26 \pm 0.07	0.33 \pm 0.04	0.20 \pm 0.03
	Modiste-KNN ($\gamma = 0.2$)	0.16 \pm 0.05	0.33 \pm 0.04	0.21 \pm 0.06	0.24 \pm 0.03	0.34 \pm 0.06	0.15 \pm 0.02
CIFAR-2A	Modiste-LinUCB ($\alpha = 0.1$)	0.15 \pm 0.08	0.30 \pm 0.04	0.14 \pm 0.05	0.32 \pm 0.02	0.31 \pm 0.05	0.26 \pm 0.07
	Modiste-LinUCB ($\alpha = 10$)	0.14 \pm 0.04	0.32 \pm 0.02	0.18 \pm 0.04	0.31 \pm 0.02	0.32 \pm 0.05	0.26 \pm 0.08
	Modiste-KNN ($\gamma = 0.01$)	0.12 \pm 0.03	0.33 \pm 0.02	0.14 \pm 0.06	0.31 \pm 0.03	0.35 \pm 0.06	0.14 \pm 0.03
	Modiste-KNN ($\gamma = 0.2$)	0.17 \pm 0.05	0.32 \pm 0.06	0.20 \pm 0.09	0.31 \pm 0.03	0.35 \pm 0.06	0.16 \pm 0.04

Algorithm		$r_{A_1} = [0.8, 0.8, 0.1, 0.1]$ $r_{A_2} = [0.2, 0.1, 0.1, 0.2]$		$r_{A_1} = [0.2, 0.8, 0.1, 0.1]$ $r_{A_2} = [0.8, 0.1, 0.1, 0.2]$		$r_{A_1} = [0.2, 0.5, 0.5, 0.8]$ $r_{A_2} = [0.8, 0.1, 0.1, 0.8]$	
		$r_h(\pi)$	$c(\pi)$	$r_h(\pi)$	$c(\pi)$	$r_h(\pi)$	$c(\pi)$
MMLU-2A	Modiste-LinUCB ($\alpha = 0.1$)	0.26 \pm 0.06	0.03 \pm 0.01	0.22 \pm 0.09	0.04 \pm 0.01	0.47 \pm 0.08	0.03 \pm 0.02
	Modiste-LinUCB ($\alpha = 10$)	0.15 \pm 0.05	0.04 \pm 0.01	0.18 \pm 0.07	0.03 \pm 0.01	0.40 \pm 0.06	0.05 \pm 0.01
	Modiste-KNN ($\gamma = 0.01$)	0.16 \pm 0.05	0.05 \pm 0.00	0.15 \pm 0.06	0.03 \pm 0.01	0.39 \pm 0.06	0.03 \pm 0.01
	Modiste-KNN ($\gamma = 0.2$)	0.15 \pm 0.03	0.05 \pm 0.01	0.12 \pm 0.03	0.03 \pm 0.00	0.38 \pm 0.05	0.03 \pm 0.01

Table 7: We vary the K and W parameters used to instantiate KNN across three datasets and report the expected risk $L_h(\pi)$ (lower is better) and expected cost $c(\pi)$ (lower is better) across 5 runs. The human simulation used here is the same as the one used in the second setting of Table 4.

	$K = 3, W = 10$		$K = 5, W = 10$		$K = 5, W = 25$		$K = 8, W = 40$	
	$L_h(\pi)$	$c(\pi)$	$L_h(\pi)$	$c(\pi)$	$L_h(\pi)$	$c(\pi)$	$L_h(\pi)$	$c(\pi)$
Synthetic-2A	0.20 \pm 0.11	0.25 \pm 0.08	0.15 \pm 0.05	0.30 \pm 0.03	0.14 \pm 0.05	0.31 \pm 0.03	0.12 \pm 0.04	0.00 \pm 0.00
CIFAR-2A	0.25 \pm 0.15	0.24 \pm 0.12	0.14 \pm 0.04	0.34 \pm 0.03	0.17 \pm 0.04	0.30 \pm 0.04	0.14 \pm 0.04	0.32 \pm 0.03
MMLU-2A	0.18 \pm 0.07	0.03 \pm 0.01	0.14 \pm 0.04	0.03 \pm 0.01	0.15 \pm 0.03	0.04 \pm 0.01	0.15 \pm 0.04	0.03 \pm 0.01

Table 8: On the CIFAR-2A dataset, we explore the effect of varying the embedding size for KNN, with $K = 8, W = 25$ (Top), and LinUCB (Bottom). We report the expected risk $L_h(\pi)$ (lower is better) and expected cost $c(\pi)$ (lower is better) averaged over 5 runs. Recall that in our main paper experiments we used two-dimensional t-SNE embeddings, not these model embeddings, for ease of visualization.

Embedding Size	$r_{A_1} = [0.7, 0.1, 0.7]$ $r_{A_2} = [0.1, 0.7, 0.1]$				$r_{A_1} = [0.7, 0.1, 0.7]$ $r_{A_2} = [0.7, 0.7, 0.1]$			
	$T = 100$		$T = 200$		$T = 100$		$T = 200$	
	$L_h(\pi)$	$c(\pi)$	$L_h(\pi)$	$c(\pi)$	$L_h(\pi)$	$c(\pi)$	$L_h(\pi)$	$c(\pi)$
2	0.18 \pm 0.08	0.28 \pm 0.06	0.14 \pm 0.04	0.32 \pm 0.03	0.32 \pm 0.05	0.24 \pm 0.06	0.33 \pm 0.06	0.23 \pm 0.05
4	0.18 \pm 0.04	0.29 \pm 0.04	0.16 \pm 0.04	0.32 \pm 0.03	0.33 \pm 0.05	0.20 \pm 0.05	0.33 \pm 0.05	0.21 \pm 0.04
8	0.15 \pm 0.05	0.30 \pm 0.04	0.15 \pm 0.03	0.33 \pm 0.03	0.32 \pm 0.05	0.24 \pm 0.04	0.33 \pm 0.05	0.24 \pm 0.06
512	0.15 \pm 0.05	0.30 \pm 0.04	0.15 \pm 0.03	0.33 \pm 0.03	0.35 \pm 0.05	0.24 \pm 0.07	0.35 \pm 0.05	0.23 \pm 0.04

Embedding Size	$r_{A_1} = [0.7, 0.1, 0.7]$ $r_{A_2} = [0.1, 0.7, 0.1]$				$r_{A_1} = [0.7, 0.1, 0.7]$ $r_{A_2} = [0.7, 0.7, 0.1]$			
	$T = 100$		$T = 200$		$T = 100$		$T = 200$	
	$L_h(\pi)$	$c(\pi)$	$L_h(\pi)$	$c(\pi)$	$L_h(\pi)$	$c(\pi)$	$L_h(\pi)$	$c(\pi)$
2	0.31 \pm 0.05	0.19 \pm 0.03	0.32 \pm 0.04	0.20 \pm 0.02	0.49 \pm 0.05	0.10 \pm 0.08	0.49 \pm 0.05	0.11 \pm 0.08
4	0.14 \pm 0.04	0.36 \pm 0.02	0.14 \pm 0.04	0.36 \pm 0.02	0.32 \pm 0.04	0.23 \pm 0.06	0.31 \pm 0.50	0.22 \pm 0.05
8	0.13 \pm 0.04	0.35 \pm 0.02	0.13 \pm 0.03	0.36 \pm 0.02	0.31 \pm 0.03	0.20 \pm 0.03	0.31 \pm 0.04	0.20 \pm 0.04
512	0.17 \pm 0.03	0.31 \pm 0.03	0.16 \pm 0.04	0.31 \pm 0.03	0.34 \pm 0.04	0.24 \pm 0.05	0.33 \pm 0.06	0.25 \pm 0.04

Table 9: We evaluate $|\mathcal{A}| > 3$ in the cost-agnostic setting, $L_h(\pi_t)$ for $t = 50, 100, 250$ for the same setup as Table 1, but with more arms. We find that `Modiste` works well over time. The success of `LinUCB` is highly dependent on the embedding space and its geometry.

Algorithm		$T = 50$	$T = 100$	$T = 250$
CIFAR-5A	Modiste-LinUCB	0.59 ± 0.10	0.29 ± 0.17	0.34 ± 0.10
	Modiste-KNN	0.19 ± 0.15	0.14 ± 0.17	0.11 ± 0.15
MMLU-4A	Modiste-LinUCB	0.13 ± 0.10	0.10 ± 0.07	0.17 ± 0.09
	Modiste-KNN	0.11 ± 0.12	0.08 ± 0.12	0.02 ± 0.04

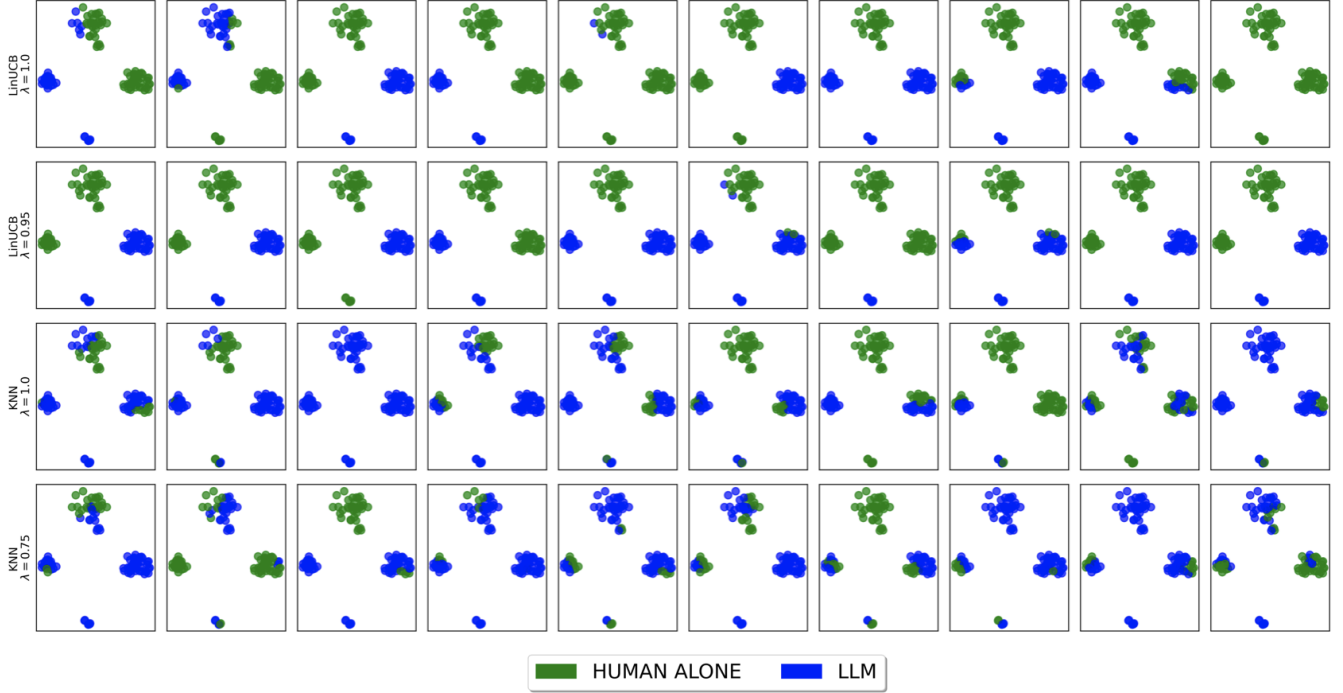


Figure 11: Snapshots of the learned decision support policies computed at the end of 60 interactions with randomly sampled users for MMLU-2A. The forms of support are colored in t-SNE embedding space. Topics correspond to clusters, clockwise from the top: math, biology, computer science, foreign policy.

Table 10: We report expected loss $L_h(\pi)$ and expected cost $c(\pi)$ incurred (lower is better) across *all* trials by Prolific participants for each Algorithm and **bold** the variant with the lowest $L_h(\pi)$. `Modiste` learns effective, low-cost policies: for CIFAR, `Modiste` outperforms all baselines. For MMLU, we find that `Modiste` learns a policy with roughly the same performance as the best offline policy but at *half* the cost. We also consider different choices of λ , where $\lambda = 1.0$ corresponds to the standard setting and $\lambda \neq 1.0$ corresponds to a cost-aware setting.

Algorithm	$L_h(\pi)$	$c(\pi)$	Algorithm	$L_h(\pi)$	$c(\pi)$
H-ONLY	0.57 ± 0.06	0	H-ONLY	0.44 ± 0.07	0
H-MODEL	0.44 ± 0.04	0.5	H-LLM	0.22 ± 0.06	0.1
H-CONSENSUS	0.32 ± 0.06	0.5	Population	0.34 ± 0.08	0.05 ± 0.00
Population	0.6 ± 0.02	0	Modiste (LinUCB, $\lambda = 1.0$)	0.26 ± 0.07	0.05 ± 0.00
Modiste (LinUCB, $\lambda = 1.0$)	0.28 ± 0.03	0.35 ± 0.01	Modiste (KNN, $\lambda = 1.0$)	0.32 ± 0.1	0.06 ± 0.01
Modiste (KNN, $\lambda = 1.0$)	0.24 ± 0.03	0.39 ± 0.04	Modiste (LinUCB, $\lambda = 0.95$)	0.31 ± 0.09	0.06 ± 0.01
Modiste (LinUCB, $\lambda = 0.85$)	0.37 ± 0.07	0.25 ± 0.01	Modiste (KNN, $\lambda = 0.75$)	0.32 ± 0.1	0.06 ± 0.01
Modiste (KNN, $\lambda = 0.75$)	0.24 ± 0.03	0.4 ± 0.03			

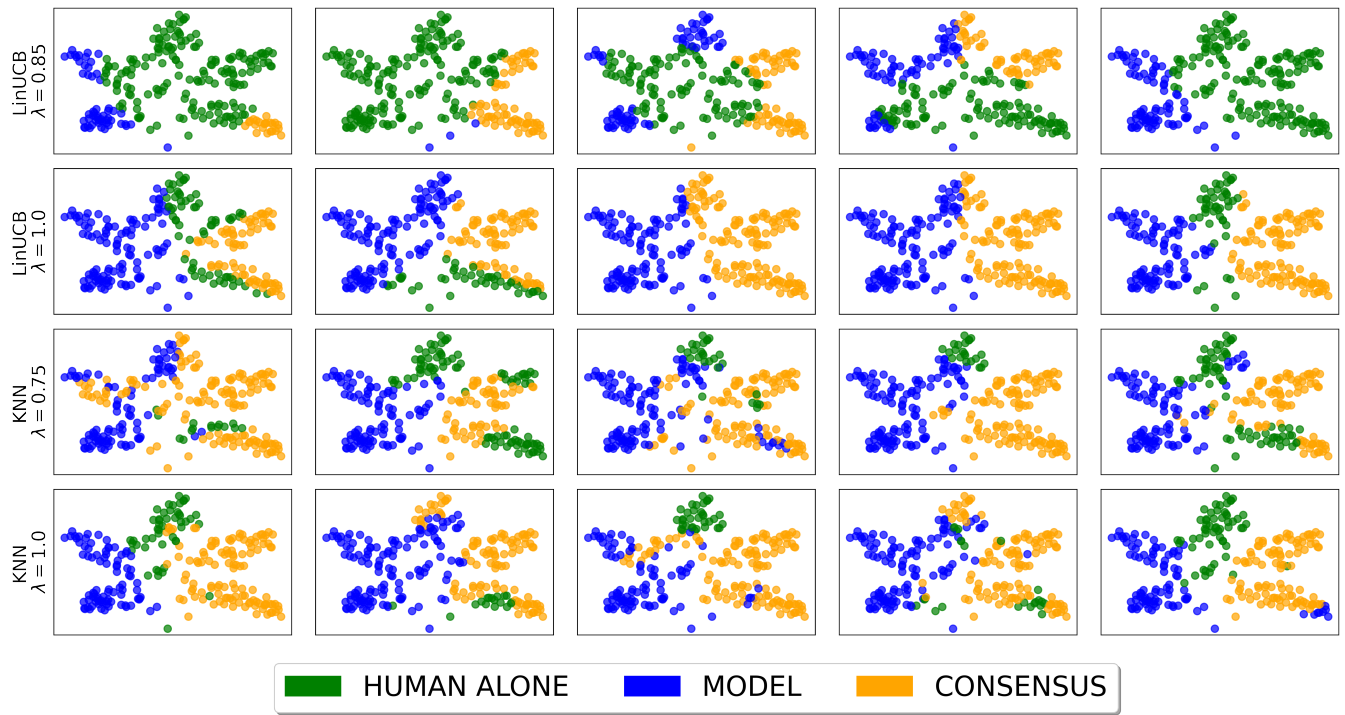


Figure 12: Snapshots of the recommended forms of support learned via `Modiste` for all participants in the CIFAR task, for different λ . Policies learned using KNN get closer to optimal; see Figure 4.